PHILOSOPHICAL TRANSACTIONS A

royalsocietypublishing.org/journal/rsta

Architecture and dynamics of magma reservoirs

Marie Edmonds[1], Katharine V. Cashman[2], Marian Holness[1] and Matthew Jackson[3]

[1]Department of Earth Sciences, University of Cambridge, Downing Street, Cambridge CB2 3EQ, UK
[2]School of Earth Sciences, University of Bristol, Wills Memorial Building, Queens Road, Clifton BS8 1RJ, UK
[3]Department of Earth Science and Engineering, Imperial College London, London SW7 2AZ, UK

Introduction

Cite this article: Edmonds M, Cashman KV, Holness M, Jackson M. 2019 Architecture and dynamics of magma reservoirs. *Phil. Trans. R. Soc. A* **377**: 20180298.
http://dx.doi.org/10.1098/rsta.2018.0298

Accepted: 16 October 2018

One contribution of 15 to a Theo Murphy meeting issue 'Magma reservoir architecture and dynamics'.

Subject Areas:
geophysics, volcanology

Keywords:
magma reservoir, mixing, mush, volatiles, melt, crystals

Author for correspondence:
Marie Edmonds
e-mail: marie.edmonds@esc.cam.ac.uk

This introductory article provides a synopsis of our current understanding of the form and dynamics of magma reservoirs in the crust. This knowledge is based on a range of experimental, observational and theoretical approaches, some of which are multidisciplinary and pioneering. We introduce and provide a contextual background for the papers in this issue, which cover a wide range of topics, encompassing magma storage, transport, behaviour and rheology, as well as the timescales on which magma reservoirs operate. We summarize the key findings that emerged from the meeting and the challenges that remain. The study of magma reservoirs has wide implications not only for understanding geothermal and magmatic systems, but also for natural oil and gas reservoirs and for ore deposit formation.

This article is part of the Theo Murphy meeting issue 'Magma reservoir architecture and dynamics'.

1. Aims and scope of the issue

This special issue arose from a Theo Murphy Discussion meeting held in November 2017. The meeting brought together petrologists, geologists, geodesists, geophysicists, fluid dynamicists and modellers to discuss how, where and in what form magmas are stored in the crust; and the implications for geohazards, for understanding fundamental Earth processes such as crustal growth, and for ore deposit formation. The meeting was sparked by a large number of new discoveries in

THE ROYAL SOCIETY PUBLISHING

the field, across a range of disciplines, and by the emergence of a number of critical localities that have been the focus of key breakthroughs. In this issue, we present chapters led by the speakers in that meeting, aimed at capturing the state of the art in our understanding of the form and storage of crustal magma bodies, while exploring critical unknowns and hence identifying fruitful targets for future interdisciplinary work. Understanding storage of magma in the crust has implications not only for reconstructing crustal growth through emplacement of plutons, and understanding the precursory signals to volcanic eruptions, but also for understanding the rheological behaviour of complex multiphase systems in crustal reservoirs, knowledge that might be laterally applied to other systems e.g. oil and gas reservoirs and ore deposits.

2. What is a magma reservoir?

A *magma reservoir* may be defined as a region of partially or wholly molten rock with varying proportions of melt, crystals and exsolved volatiles [1]. Sparks *et al*. define a magma reservoir as 'the domains within the magmatic system that contain melt (± exsolved fluid) and by definition are above the solidus' [2]. Some authors have suggested that parts of the magma reservoir may be entirely below the solidus temperature, in 'cold storage', and are later rejuvenated [3]. The parts of the reservoir which contain sufficiently high crystal contents to form a semi-rigid framework may be termed 'mush' [4]. Likewise, pockets or bodies of melt with a very low (or zero) crystal fraction may exist in magma reservoirs, formed through melt expulsion from a mush, through compaction [5,6], convective or diffusive exchange or gas-driven filter pressing [7,8], or as super-liquidus melts injected into more crystal-rich material (a mush or solid country rock), which then cool and crystallize. In some systems, the 'reservoir' may span the vertical extent of the crust (and perhaps beyond, into the mantle); and may be termed a 'trans-crustal mush system' [2,9,10]. In other magmatic systems e.g. Iceland [11–14], there may be multiple, 'stacked' storage areas for magma [15], separated by subsolidus material, which has been well constrained both petrologically and geophysically [13,16] (figure 1).

Sparks *et al*. [2] review the history of the 'magma chamber' concept, whereby a liquid vat of magma slowly cools and crystallizes to produce layers of igneous minerals reflecting the liquid line of descent, to a greater or lesser degree affected by mixing and/or assimilation processes. As our observations of magmatic systems have improved, the community has acquired abundant evidence to suggest that large volumes of melt are not currently present in the crust and instead, melt may be disseminated in mush regions, and extracted shortly before eruptions [2,9,17]. Much of this paper, and the papers which follow, lay out this evidence.

The different types of regions in a magma reservoir (mush, melt, rock) have vastly different rheological and physical properties, including their viscosity [18], their response to applied stress [19–21], and their conductivity [22,23]. Sparks *et al*. [2] delineate rheological domains for the magmatic system components and show that their effective viscosities may span 25 orders of magnitude, and consequently the timescales on which reservoir processes operate range from seconds to millenia [2]. The inherent instabilities generated from the heterogeneity of the magma reservoir may give rise to scenarios whereby the reservoir may re-organize [17] or overturn [24,25] on short timescales prior to, or during, eruption. This reorganization may take place in response to a tipping point caused by the long-term processes of fractionation, settling, compaction, reactive flow and second boiling [26]; or it may be triggered by recharge of the reservoir by mafic magmas from the lower parts of the crust, or from the mantle [27–30]. In some instances magma reservoir perturbations, and sometimes eruptions, may occur in response to tectonic forcing [31].

What is the ultimate fate of the melt in magma reservoirs? Magma reservoirs may feed eruptions; or they may freeze and become plutons. Between 80 and 90% of magma supplied to the crust is emplaced endogenously [32,33], making pluton formation the most probable endpoint for much of the magma reservoir mass [34,35]. Plutonic rocks exposed at the surface provide a wealth of information about the emplacement mechanisms and differentiation processes of magma reservoirs in the crust [36,37] (figure 1).

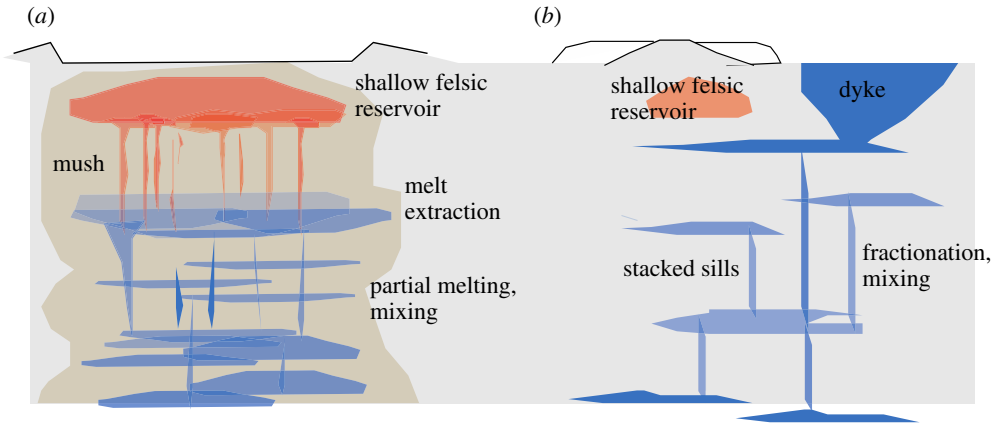

Figure 1. Schematic cartoon of the magma reservoir end-member types that may exist in (*a*) continental and arc settings [38] and (*b*) in Iceland (discussed in text) [39].

3. Evidence for the vertical extent and form of magma systems

To understand magma storage in the crust, we might wish to know the depth at which magma is stored, and for how long. What fundamental processes are occurring inside a magma reservoir as it cools and is recharged? Can we find evidence of these processes both in the erupted rock and in the geophysical signals we can measure at the Earth's surface and buried in boreholes?

In the brittle crust, magma may be emplaced along structural features such as large-scale faults [40,41], forming aligned, large composite batholiths, e.g. Rum, Arran, Adamello [42,43]. Examples of volcanic systems which are influenced by the tectonic stress field are many: e.g. lava domes in the southern parts of Monserrat are aligned parallel to the bounding faults of the half-graben extending the southern part of the island [44]; lava domes outside the Long Valley caldera emplaced parallel to regional extensional faults; and volcanoes aligned along transcurrent faults in the NW Bicol volcanic arc, Philippines [45,46]. Extreme cases of tectonic control on magma emplacement are provided by rift volcanoes, where magmas ascend through brittle faults in the continental crust associated with rifting, forming scoria cones along the rift margin and central volcanoes along the rift centre [47]. At many volcanoes, CO_2 and He emissions are concentrated along faults around volcanoes, such as caldera faults, but are also emitted from cross-cutting large-scale faults related to regional tectonics [48]. Biggs & Annen [49] explore the tectonic controls on magma emplacement.

Seismology is an important tool to study the storage and transport of magma, in real time, reviewed by White *et al*. [11]. Microseismicity occurs when rock fractures in a brittle fashion in cool crust. Not all magma movement is captured by earthquakes, however: once a magma-filled channel is 'opened' it may permit aseismic flow; likewise hot crust is ductile and does not fracture under commonly accessible strain rates [11]. In Iceland, crustal thickness ranges from 20 to 40 km [50] and the brittle part of the crust extends down to 6–8 km [11]. Seismic tomography studies of central volcanoes in Iceland have discovered magma storage areas at depths of 3–6 km and deeper. For example, at Askja volcano, a series of high V_p/V_s ratio bodies indicate the presence of melt situated at discrete locations throughout the crust to depths of over 20 km [16], consistent with the model of stacked sills [15] (figure 1). A dominant anomaly at 6 km depth cannot be the signature of crystal-poor melt, however, because it transmits shear waves, raising the possibility that this body may be mush-dominated [11]. Deeper in the crust, at up to 25 km, earthquakes have occurred in the same regions for over a decade, indicating persistent magma supply into sills, where the earthquakes occur at the sill tips, where the stress is highest [16].

Deeper in the crust, microseismicity can pick out the path of magma movement. Several years prior to the Icelandic Bárðarbunga eruption in 2014, for example, earthquakes occurred at depths

of 7 and 22 km on the SE flank of the caldera (not directly beneath it) [51]. Although the storage region beneath the caldera is thought to be at 5–12 km bsl [52], earthquakes do not occur deeper than approximately 8 km [53]. These observations show that, at least sometimes, magmas may bypass the shallow magma reservoir as has also been suggested for many other volcanic systems, based on petrology, e.g. Kīlauea and Mauna Loa, Hawaìi [54,55] and on ground displacements [56,57].

Seismicity provides an enormous amount of information, from the distribution, size and timing of the earthquakes and from the focal mechanisms, and has led to new insights about how magma is stored in sills and migrates upward in deep dykes beneath Iceland [11]. For example, a non-eruptive seismic swarm beneath the volcano of Upptyppingar occurred on a fault plane parallel to the dip and strike of the dyke (as opposed to 30 degrees to the dyke tip, which was expected). This observation, and the presence of both reverse and normal fault plane solutions, has produced a model for this swarm of repetitive melt freezing and fracture in the brittle part of the crust [58,59]. Furthermore, bursts of seismicity above the dyke may record the release of CO_2 from the ascending magma [60]. Volatile release associated with magma transfer may be a common process [11] and has also been observed at Mammoth Mountain, inside Long Valley Caldera, California [61].

Seismic tomography studies have imaged bodies with slow p wave velocities and low V_p/V_s ratios (which may represent melt-bearing regions of the crust). A region containing 10–12% melt has been imaged at depths of 4 and 6 km beneath Mount St Helens, inferred to be the top of a reservoir that extends down to 14 km depth [62]. At Nevado del Ruiz volcano (Colombia), a recent study has imaged high V_p/V_s at depths of 2–5 km, which has been proposed to indicate degassing and the presence of an exsolved volatile phase (see §5) [63]. Average melt percentages of 5–15% have been suggested for the upper crustal magma reservoir that underlies the Yellowstone caldera [64,65].

Importantly, tomography yields an averaged view of the seismic velocity structure and relies on broad seismic wavelengths of hundreds of meters to hundreds of kilometers, thereby limiting the spatial resolution. Even with dense seismometer networks, it is a challenge to image upper crustal anomalies $<\sim 5\,km^3$ or features much less than 10 km across [38]. Erupted magmas typically contain greater than 50% melt, which raises the question: can eruptible magmas hide within a crystal mush that is 85%–95% solid [38]? A region containing 5–15% melt when, viewed at a large scale, could actually contain isolated lenses rich in melt instead of the melt being broadly disseminated in small pores throughout. Are isolated bodies of melt separated by mush, or by subsolidus rock? Seismic tomography is rarely capable of resolving the difference between larger (but still less than 100 m) sill-like bodies set in a rock matrix, from a bulk mush containing a small fraction of melt in its pore space [12,66].

Magnetotelluric surveys provide complementary information; they measure directly the conductivity of the crust (and perhaps upper mantle, depending on the geometry of the survey). This method is therefore highly sensitive to the presence of melt [66–68], due to the effect of temperature on conductivity [23], as well as the presence of low density fluids, including brines [69]. Recent studies have identified signals that suggest elevated melt fractions in regions extending laterally 10s–100s km in the Cascades [70], Afar [71], Uturuncu Volcano [67] and Vesuvius-Campi Flegrei [72], perhaps suggesting that magma reservoirs may be linked up under volcanic regions, and significant magma storage may take place in the mid-crust, the lower crust or straddling the Moho.

Magma intrusion and eruption (i.e. magma addition to, and withdrawal from, the crust) is associated with inflation and deflation of the Earth's surface [73,74], reviewed by both Segall [73] and Biggs & Annen [49]. Pressure changes in magma reservoirs may be inferred from displacements of the ground surface, which may be measured in a range of ways. The rate of decay of deformation with distance reflects the centroid depth of the magma source region [73–75]. Furthermore, the amplitude of the ground displacement signal is related linearly to the pressure change, or volume change of the reservoir [73,76]. Independent constraints are required to quantify one or both of these parameters. The relative magnitude of vertical versus horizontal

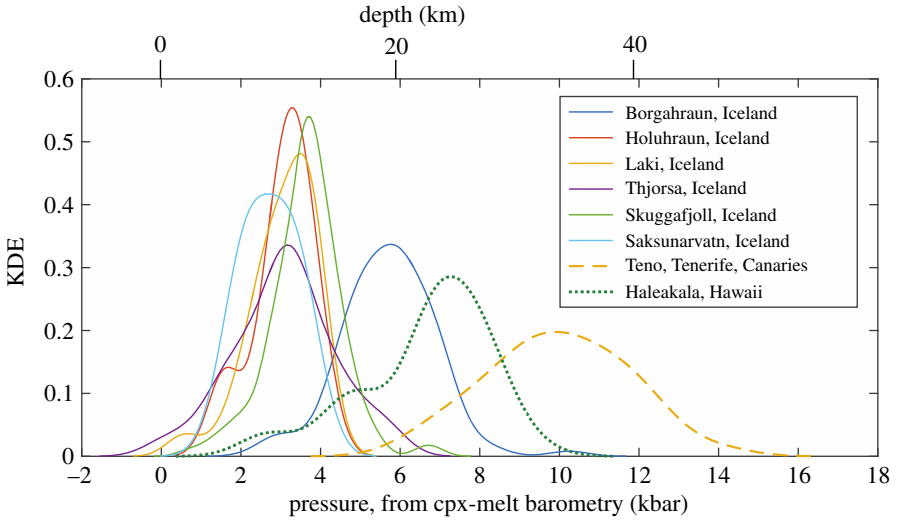

Figure 2. Last equilibration pressures of magma from clinopyroxene-melt barometry [88,89] for a range of ocean island volcanoes [88,90–95].

displacements gives information about source shape [75]. A wealth of new data, particularly from space-based measurement systems such as InSAR [76], have allowed the construction of an unprecedented, detailed record of ground deformation around volcanoes [49,56,77–80]. A number of important generalizations have been made from the overview of deformation data. The Mogi model [81] has been the mainstay of deformation modelling for several decades, and does a surprisingly good job at reproducing the deformation observed at many volcanoes. The assumption implicit in this model is that the crust is elastic. For many eruptions, however, patterns in surface displacements do not fit a simple Mogi model and multiple, complex sources (involving sills, dykes and multiple point sources) are required to fully reconcile all of the observations [74,79,82–84]. Segall [73] explores whether models involving a viscoelastic crust may be more suitable in some cases for modelling volcanic deformation (see later). It may even be possible to begin to reconcile models of complex magma reservoirs comprising regions of mush hosting multiple melt lenses, with surface observations [76].

Petrological studies of erupted magmas use barometry to place constraints on the depth of magma storage. For mafic magmas, 'OPAM' barometry uses the melt composition that is in equilibrium with plagioclase, clinopyroxene and olivine to estimate a pressure of 'last equilibration' [85,86]. Yet another method uses the density of fluid inclusions trapped inside crystals, which is proportional to pressure [87]. Figure 2 contains a summary of data from clinopyroxene-melt barometry on basalts from a range of volcanoes [88,90–95], and shows that magmas may be stored (and last equilibrate with melt prior to eruption) at great depth in the crust, close to and beyond the seismic Moho in some cases.

Barometry of numerous Icelandic eruption products has shown that melts are stored over a large range of depths in the Icelandic crust [12,88], reviewed by Maclennan [12]. Petrological barometry estimates produce some agreement with the seismic constraints on magma storage [11]. For example, clinopyroxene-melt pressures for Askja basalts typically average 2–3 kbar (6–9 km bsl) [93], a depth range that agrees well with the location of the main magma storage area deduced from seismicity [11,16]. Overall the data for Iceland are consistent with models of stacked sills throughout the crust and spanning the Moho [13,15,96,97]. During eruption, magmas may be tapped from either shallow storage areas, in the case of the central volcanoes, or from deeper for off-rift eruptions. It is important to note, however, that the petrological features of erupted rocks are a palimpsest of many processes acting over timescales of 10^0–10^4 years, perhaps entraining crystals from multiple reservoirs with different histories [12], as well as being on a much smaller

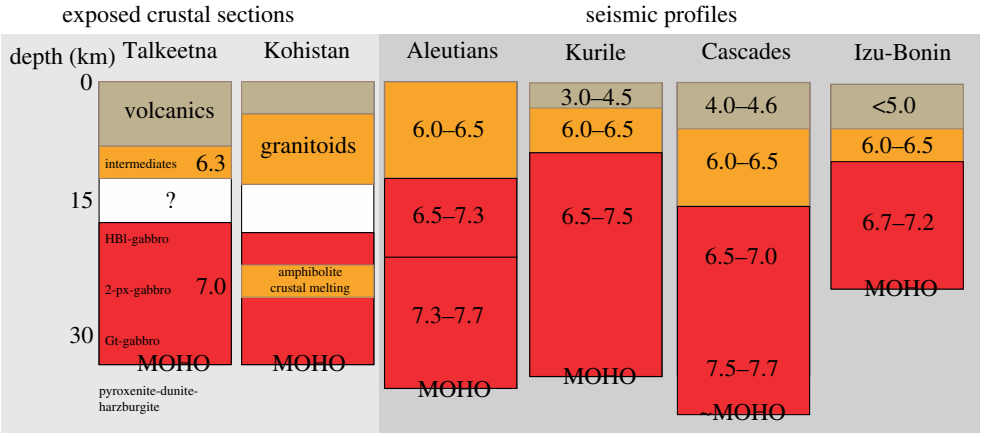

Figure 3. Schematic sketches of exposed arc sections of Talkeetna (Alaska, USA) and Kohistan (Pakistan) [98]. Brown represents volcanic rocks, orange are intermediate to felsic plutonic rocks [53–72 wt% SiO_2], red is mafic lithologies (gabbro cumulates) [98]. The Moho is defined as the transition between ultramafic rock (plagioclase absent) and gabbroic rock (plagioclase present). The right-hand four sections are a summary of seismic velocities for a range of arcs [98]: Aleutian [99], Kurile [100], Cascade [101] and Izu-Bonin [102].

spatial scale (micrometres to centimetres) than geophysical observations (which are over metres to kilometres): therefore, it is extremely challenging to link these two data sources.

Exposed crustal arc sections allow direct insight into the structure of the magmatic system preserved beneath volcanic arcs and clues about depths of magma storage and differentiation (figure 3). The most complete of these sections are Talkeetna (Alaska) and Kohistan (Pakistan). Talkeetna is an example of island arc crust, active between 200 and 160 Ma [103]. The lower part of this crust is made of pyroxenites and garnet-bearing gabbros; hornblende gabbro-norites in the mid-crust, gabbroic rocks and intermediate-felsic plutonic rocks in the middle-upper crust, and volcanic rocks in the uppermost crust (approx. 7 km thick), intruded by felsic to intermediate tonalites and quartz diorites [98]. These upper crustal plutonic rocks crystallized at 0.13–0.27 GPa (5–9 km) [104]. Kohistan is a section of island arc crust obducted during India-Eurasia collision [105]. The lowermost part of the crust is ultramafic and consists of garnet-gabbros (granulites) that overlie and intrude the residual/cumulate rocks of the subarc mantle [106]. The middle crust of the arc is separated into a northern section (middle crust represented by calcalkaline plutons of the Kohistan batholith) and a southern section (middle crust represented by metadiorites, metagabbros, metasediments, and metavolcanics of the Southern Amphibolite Belt) [98,107]. The shallowest part of the arc section consists of volcanic, sedimentary, and shallow-level granitic rocks in the northern part of the exposure [98]. The Famatinian magmatic arc in western Argentina is a differentially exhumed section of a Late Cambrian-Middle Ordovician arc formed by plate subduction beneath the Gondwanan margin [108]. Here, the source zones of tonalites and diorites are located at the boundary of a lower, gabbro-dominated portion of crust and an upper intermediate unit. The intermediate rocks are sourced from mafic intrusions, melting of metasedimentary rocks, forming a leucotonalitic vein and dyke system that coalesces to form leucotonalitic or tonalitic magma bodies. The preserved textures are migmatitic and may reflect melts caught in the act of segregation [108]. Alternatively, these rocks may represent 'failed' source regions, from which the melt did not escape efficiently.

Figure 3 shows a summary of the main features of such sections, as well as some seismic velocity data from modern arcs. In all cases, high-density mafic and ultramafic lithologies are present in the lower crust, which may represent cumulates; with intermediate and felsic plutonic and volcanic rocks in the mid and upper sections. In both exposed cases shown here, there is evidence for fractionation of melts beneath the Moho (defined as plagioclase-in), manifest

as dunite and pyroxenite cumulates; the latter is the dominant lithology near the Moho [98]. Above the Moho, gabbroic (olivine-free) cumulates dominate, which formed at 0.5–1.0 GPa [104]. Geochemically, the upper intermediate and felsic magmas can be related to the lower ultramafic portions by fractional crystallization, suggesting that felsic liquids segregated from mafic cumulate mushes and ascended to shallower levels, creating stable density stratification. In the exposed sections, there is abundant evidence for crustal melting, with migmatites and tonalite melts produced from the partial melting of metasediments [108]. In all of the exposed sections, the mid-crust is highly heterogeneous, with host amphibolite and multiple types of magmas present in close proximity and is likely a region of extensive mixing and mingling, and assimilation.

In general, the features of the exposed arcs are consistent with the results of seismic studies of modern arcs [109] (figure 3), which show distinct seismic velocities for upper, mid and lower crust. The most variability, in both velocity and thickness, occurs in the mid-crust, where gabbroic as well as felsic rocks have been inferred. Seismic velocities of the lower crust in modern arcs are consistent with granulite facies rocks [110], but are thought to be highly dependent on the water content of melts in the lower crust [111]. Models to describe how these arc sections evolve with time typically involve a young arc crust dominated by fractionation and mixing/mingling, followed by a second stage, once the arc crust is much thicker, which is characterized by extensive crustal assimilation [109].

4. Magmatic processes in reservoirs

(a) Liquid vats versus crystal mush: evidence from microstructures

There is abundant evidence that liquid-rich magma bodies have existed in the past and may exist locally on small scales today. Such a melt-rich body may cool through inward solidification, generating a progressive layering (from mafic to more evolved bulk compositions) by efficient separation of crystals from the remaining liquid [4,112–114], perhaps interrupted by recharge events which reset the bulk composition and temperature, or 'sedimentary' features such as stopped and settled blocks and gravity currents involving crystal-rich suspensions [115,116]. Fractionation by gravitational settling of crystals can generate a sequence of modal types and crystal sizes on the floor of the 'chamber' [4,112,117]. Crystals may orient in the settled layer from either compaction or alignment due to flow or shear at the crystal–melt interface [118–121]. Examples of such features exposed at the Earth's surface are present in the Skaergaard intrusion [116], and the Rustenburg Layered Suite of the Bushveld Intrusion [114]. For small melt bodies, such as sills, it is even possible to infer the presence or the absence of, and the strength of, convection based on the stratigraphic distribution of grain size of the crystals at the upper and lower surfaces of the intrusion [122].

The other end member of magmatic storage is where magmas are stored on long timescales as a crystal-rich mush [1,2,9,112,123,124]. In this scenario, liquid-rich regions form by either expulsion of melt from the mush pile during compaction [5,6] or gas-driven filter pressing [7], and may be enhanced by partial melting of the mush during reharge by hotter magmas [22,29,125,126]. Under these conditions, phenocrysts initially grow suspended in a liquid, but may experience protracted periods of storage and further crystal growth in the mush. Is there evidence for this latter scenario in erupted rocks? Holness *et al.* [127] show it is possible to 'decode' the microstructural features of plutonic rocks and crystalline enclaves or xenoliths erupted in volcanic rocks to infer the environment in which the crystals formed [117,128]. The aspect ratio of plagioclase crystals, for example, records the amount of undercooling experienced by the magma during growth [129] (figure 4). Dihedral angles, in contrast, are affected by cooling rate: during rapid crystallization grains impinge upon one another with planar faces, which generate a wide range of disequilibrium dihedral angles and resulting in a high total interfacial free energy [130,131]. At low cooling rates, crystal–melt boundaries can evolve towards the curved interfaces indicative of low interfacial free energy, with equilibrium dihedral angles at two- and three-grain junctions. In this way, the characteristic microstructures of plutonic xenoliths in volcanic systems can be

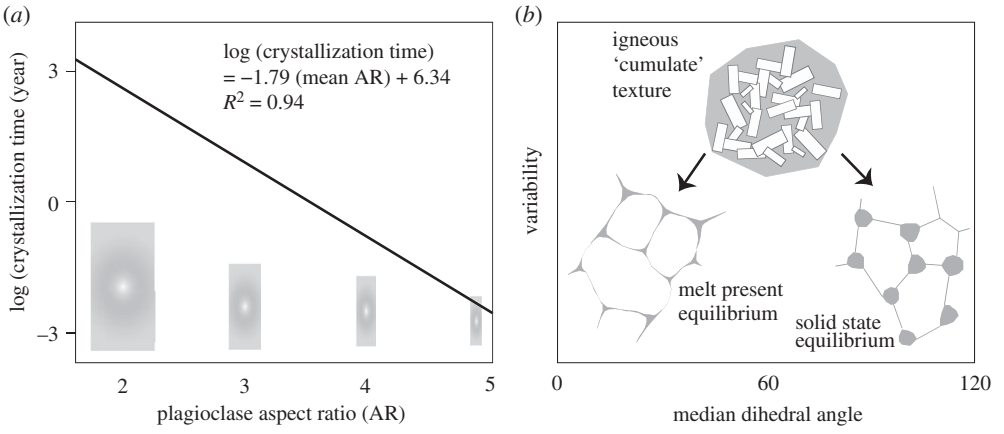

Figure 4. Petrological tools to decode microstructure. (*a*) Plagioclase aspect ratios may be used to estimate cooling rates in volcanic and plutonic rocks [129]. Dihedral angles of approximately 60° are characteristic of textures arising from igneous processes (impingement), arising from crystal settling, which may equilibrate with time in the mush pile [130,131].

interrogated to assess whether their constituent grains formed in a liquid-rich environment or *in situ* in a mush [127]. Such microstructural evidence points towards the existence of liquid-rich fractionating sills of thicknesses up to approximately 800 m for some Galapagos volcanic plumbing systems (Wolf and Ecuador volcanoes) [127].

A common feature of many volcanic deposits is the occurrence of polyphase crystal clusters, or glomerocrysts [132–135]. These may be fragments of disaggregated crystal mush that has experienced open system mixing (see above; refs), or they may arise from synneusis [136]. The mechanisms and likelihood of crystal clustering arising from these processes are evaluated by McIntire *et al*. [137].

(b) Mush processes: recharge, reactive flow, disaggregation, segregation and mingling

There is now abundant evidence from erupted magmas in all settings for both fractional crystallization and mixing; indeed it appears that mixing is near-ubiquitous [3,138], reviewed by Cashman & Edmonds [139]. Phenocrysts grown during fractional crystallization as grains suspended in the liquid are commonly euhedral and have rims, and perhaps cores, in equilibrium with the carrier liquid. Antecrysts, in contrast, may display disequilibium features such as rounding and resorption, reverse zoning or compositionally stepped rims. Antecrysts picked up from crystal layers, or mush, can be identified texturally by their deviations from linear on crystal size distribution plots [39,140], and sometimes by deformation textures such as dislocations [141]. Trace element systematics of antecrysts may show trace element concentrations that are not in equilibrium with the carrier liquid, but are in equilibrium with a related liquid from the same magmatic system [142,143]. The clear evidence that whole rock compositions merely represent an 'average' composition means that to really understand the processes of hybridization and the tempo of magma assembly, one must turn to microanalysis of the components.

An example of extensive antecryst incorporation comes from Kīlauea Volcano, where the cores of olivine macrocrysts are commonly not in equilibrium with their carrier liquids [54]. Instead, olivine cores are usually more primitive, indicating that they were 'picked up' from some (less evolved) part of the magma reservoir. Comparison of summit and rift magmas, erupted both effusively and explosively, shows that the Kīlauea magma reservoir is compositionally zoned, and that large volume eruptions excavate deeper into the reservoir system and therefore erupt more primitive olivine compositions, as well as more mafic (hotter) melt [55]. The most primitive olivines at Kīlauea are also typically the largest, and show evidence of dislocation creep during

deformation, suggesting they formed part of a mush system beneath the summit caldera subject to loading and/or shear [144].

Other volcanoes show some of the same features, suggesting that magma mixing, and perhaps disruption of crystal mushes to entrain their more primitive crystals, is a common process beneath active volcanoes [139]. Icelandic magmas, for example, have olivine-hosted melt inclusions that are related geochemically to the liquid that carried the crystals to the surface [145], reviewed by Maclennan [12]. Thus even though the crystals themselves are out of equilibrium with the carrier liquid, the melt inclusions record an earlier history of melt ponding and cooling. This is further evidence that the crystals are antecrysts that are related to the liquid by fractionation but are not in equilibrium with that liquid. One interpretation of these observations is that magmas in Iceland do not interact with mush systems other than their own on the way to the surface [12], consistent with microseismic evidence of brittle fracture accompanying melt migration between sills [11].

Trace element signatures in olivine-hosted melt inclusions can further be used to constrain the dimensions of the magma bodies in which they were formed. If the variability in trace element ratios and isotopic ratios in the melt inclusions is inherited from mantle-derived heterogeneity [145,146], then the melt inclusions were trapped during concurrent cooling and mixing [145]. Thermal models for sill cooling, convection and mixing, coupled with thermodynamic models of fractionation, place constraints on sill thickness. It emerges that these magma bodies must be less than 10 m thick to produce the observations [12], which involves the production of a 4 m thick layer of mush over a timescale of approximately one month, reviewed by Maclennan [12].

Evidence for antecryst entrainment is not restricted to basaltic volcanic centres, but instead are common features of rhyolites from caldera-forming eruptions in continental settings [147] as well as a range of magma types in arc settings [148,149]. In fact, arc magmatic systems preserve clear evidence for extensive mixing and mingling in the form of resorption textures, sieved plagioclase, antecrystic clots and clusters, mafic enclaves and other signs of disequilibrium [132,133,150–154]. Cashman & Edmonds [139] explore the heterogeneity in major elements of arc melts (glasses) inherent in magma extracted from different pressures in the arc crust, which record different liquid lines of descent owing to the influence of H_2O on the crystallization path.

The minerals in intermediate arc magmas also record information about magma petrogenesis that can be used to infer the compositions of melts that existed earlier in the magma's history. One example is evidence for 'cryptic' crystallization of amphibole at depth that is later 'erased' from the system through mixing and fractionation during magma ascent [155]. Humphreys *et al.* [138] use amphibole compositions, which hold a large range of trace elements and are stable over a large pressure range, to infer deep crustal mixing and differentiation of andesites [138]. The composition of 'amphibole equilibrium melts' (AEMs) may be calculated using trace element partitioning schemes [138]. The amphiboles preserve a record of multiple interactions (mixing episodes) between mafic melts and evolved melts (dacites); differences in the AEMs and whole rock compositions, in particular, reflect assimilation of plagioclase and zircon.

Mid-ocean ridge environments (both fast- and slow-spreading) may also be underlain by extensive regions of mush [156], although the presence and significance of mush beneath mid-ocean rudges is debated [12]. Mid-ocean ridges are ideal settings to study magma storage and the importance of crystal mush: MOR basalt compositions are well understood and reasonably uniform [157,158]; there is abundant geophysical imaging data [156]; and ophiolite sections allow characterization of the layering and structure through the entire crust [96]. These different data streams do not yet provide a single interpretation of magmatic processes. One view is that melt ascends through the mush through porous flow, driven by buoyancy and through expulsion by compaction [5], rather than by dyking. As melts ascend, they will inevitably flow through material with which they are not in chemical equilibrium, as reviewed by Lissenberg *et al.* [159]. This will manifest (on a grain scale) by evidence of reaction such as dissolution, symplectites, reaction rims or complex mineral zoning. Geochemically, reactive flow will be recorded in the trace element zoning in crystals close to the channels of melt movement [159,160], giving rise to heterogeneous and trace element-enriched melt compositions. These melts may mix and homogenize during flow, leaving Mg# relatively unchanged; they may also entrain diverse phenocrysts and antecrysts

from the mush during transport. Reactive flow also helps to explain the origin of the vertical fabrics observed in ophiolites [161]. Reactive flow may involve both evolved and more primitive melts, and the extent of reactive homogenization in a single mush body depends on allowable diffusion time scales. The resulting range of textures, zoning and compositions thus produced allow reconstruction of the range of melt compositions produced during reactive flow [159]. An alternative view arises from examination of exposed ophiolite sections in Oman, which led Korenaga & Kelemen [15] to conclude that the cumulate rocks of the lower crustal section formed in small, open system melt lenses, and that melt flux through the mush was not important in supplying the total melt flux for the system. Taken together, outstanding questions surround the importance of reactive porous flow in mush systems beneath MORs.

5. Time-dependent nature of magma reservoirs

Important questions about the behaviour of magma reservoirs concern the timescales of various processes, reviewed by Cooper [162]. These timescales are important in evaluating volcanic hazards, interpreting volcano monitoring data and, on longer timescales, developing models of likely repose periods for large volcanic systems. The timescales of magma supply, fractionation, mixing and recharge events also have relevance for broader questions relating to the timescale of crustal growth and of the creation of ore deposits in the crust. We might ask: how long does it take to make a magma reservoir? How long are magma reservoirs active? And of that time, how long are they super-solidus? On what timescale are magmas remobilized and 'assembled' prior to eruptions? How fast are melts extracted from mushy regions to form eruptible liquid volumes?

Progress in developing methods and models to generate timescale data in magmatic petrology, is reviewed, along with their limitations, by Cooper [162], as well as by other authors [163,164]. Diffusion modelling of compositional steps in volcanic crystals has emerged as a critical method to establish the age of 'young' (10^{-1}–10^{3} years) mixing events in magmas [165,166], made possible by advances in microanalysis as well as in modelling diffusional processes. Most commonly modelled are the coupled diffusion of Fe and Mg as well as Li, Sr, Mg and Ba diffusion in plagioclase [167]. Importantly, the timescale recorded by the diffusive relaxation of a compositional profile in a mineral is a function of temperature, and as such may record only a fraction of a mineral's total age [3]. When combined with other petrological methods, diffusion chronometry becomes even more powerful. Diffusion chronometry on crystal cargoes erupted in Iceland, combined with barometry, shows that, at least in some cases, magmas may rise rapidly (approximate days) from crustal storage areas, which may be deep (approx. 20 km; [168]). These short timescales almost certainly require a brittle rock matrix and the opening of dykes, consistent with microseismicity observed in Iceland [11] (figure 3).

Radiometric dating systems, such as U-Pb and U-series of accessory minerals such as zircon and titanite [164,169,170], record longer ages, corresponding to the time because the mineral fractionated parent isotopes and became closed. Such a radiometric 'clock' operates only below its closure temperature. Crystallization ages of the minerals in magmas erupted from volcanoes are 10^{4}–10^{5} years [162]. Remarkably, this entire age span can be recorded by the growth zones of individual crystals (commonly zircon), showing that magma reservoirs can be very long-lived.

This diverse sampling of timescales records different aspects of the system (figure 5). The shorter, diffusional re-equilibration timescales tell us about mixing and magma ascent prior to eruption [171]. Multiple subsets of crystal populations, and multiple zones inside crystals, may allow the reconstruction of complex series of mixing events that involve different populations of crystals [165,172,173]. In general, the shorter timescales are generated in the more mafic systems, suggesting that mixing occurs closer to eruption, perhaps consistent with the lower viscosity and higher flow rates of such systems. Older ages derived from the radiometric dating of crystals, in contrast, tell us about the longevity of the reservoir and the timescales of crystallization (figure 5). In tandem with thermal modelling, the integrated picture, from many volcanic deposits worldwide, shows that magmas spend much of their time close to or even below their solidus temperatures, and are heated in short bursts, which may or may not result in eruption [3].

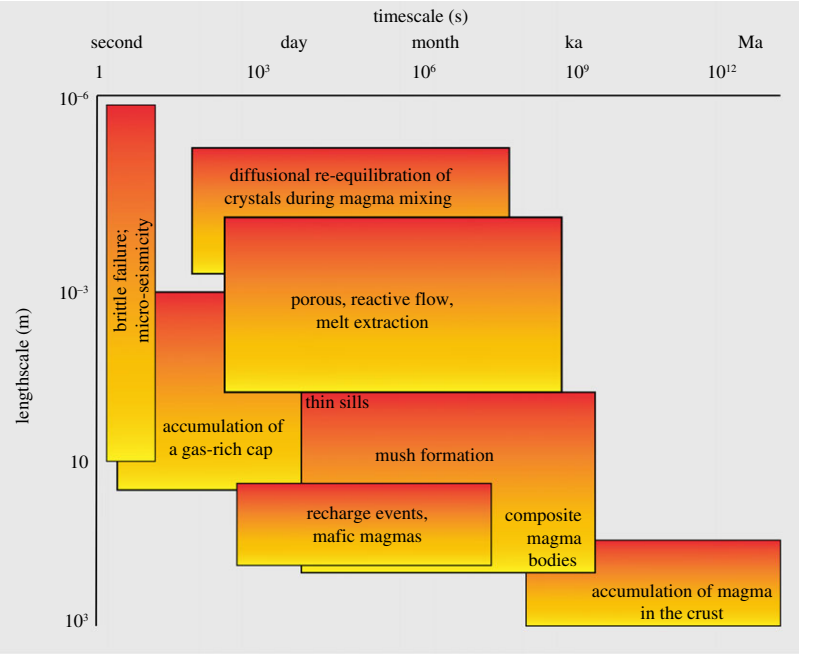

Figure 5. Time- and lengthscales associated with different magmatic processes in the crust; discussed in the text.

6. Importance of the exsolved volatile phase

Volatiles typically make up only a few wt% of magmas in the crust, but they have enormous importance in controlling phase equilibria, buoyancy, and physical and rheological properties of magmas, including the mush [174–177]. In magma reservoirs in the crust, dissolved volatiles exsolve if fluid saturation is reached [178], where the confining pressure becomes equal to or less than the sum of the partial pressures of volatiles in the melt. Fluid saturation may occur during decompression (first boiling) or during isobaric crystallization (second boiling). Second boiling dominates in magma reservoirs, producing an exsolved magmatic volatile phase (MVP) that is initially rich in CO_2 and becomes more hydrous as crystallization proceeds (see Edmonds & Woods [177] for a review). Evidence for the existence of an MVP in magma reservoirs includes: miarolitic cavities in plutonic rocks [178], magma compressibility inferred from muted ground displacements ([179–182], and the existence of low V_p/V_s regions beneath calderas such as Yellowstone [183].

How does this exsolved volatile phase behave in magma reservoirs, particularly in the mush-dominated portions of such reservoirs? Degruyter *et al.* [176] review the various regimes that may allow the MVP to outgas from crustal magma reservoirs, building on previous work building numerical models at the pore-scale of how gas may migrate through crystal-rich magmas [22,126,176,184,185]. Channel flow by viscous fingering may occur in a permeable crystal network at intermediate melt fractions [186,187]. For crystal fractions that exceed the 'locking point', high overpressures are required to overcome the strength of the crystal framework to propagate fractures through the mush to allow outgassing [186], which may be possible at low pressures. In melt-rich lenses in the magma reservoirs, in contrast, the MVP may get 'held up' during relatively slow Stokes' rise of bubbles [185,188], such that melt lenses may be areas in which MVP can accumulate; this process may be the basis of the formation of gas-rich caps to magma reservoirs.

It follows then, perhaps rather counterintuitively, that gas-rich regions may develop in the shallow reaches of magma reservoirs, because of the relatively fast migration of the MVP through

the crystal-rich regions, and accumulation in the melt lenses [185]. This mechanism might explain the large emissions of volcanic SO_2 that often accompany explosive eruptions [181,189–193], the persistent degassing between eruptions [194] and the formation of hydrothermal ore deposits in the roof zones of magma reservoirs [195]. 'Gas-rich caps' may be the primary cause of ground displacements, with outgassing causing subsidence, and inputs of magma fluids into a hydrothermal system generating cyclic uplift and subsidence, e.g. for Aluto, East African Rift and Campi Flegrei, Italy [196,197]. Outgassing of accumulated exsolved volatiles in the upper parts of volcanic systems may even generate downward-propagating instabilities which might induce mixing and mingling [17], or even eruption [198]. The MVP may also play an important role in generating melt lenses in crystal mushes, particularly in the upper crust, where gas-driven filter pressing may cause expulsion of melt from a crystal framework because of expansion of the MVP phase during second boiling [7]. Additionally, if an MVP develops in a crystal mush, it greatly alters its rheological properties, allowing it to be rapidly remobilized [8,19,20].

Figure 6 shows a compilation of basaltic melt inclusion water contents. The melt inclusions trapped melt prior to (most of) the degassing of water. The data show that pre-eruptive melt water concentrations may vary between 0.1 and 0.3 wt% (for mid-ocean ridges and relatively dry ocean island melts) up to 3–6 wt% for arc basalts and some wet ocean island melts (e.g. Canaries). The water content of melt, which varies with tectonic setting (figure 6), probably exerts an important control on the architecture of magmatic systems [139]. In relatively dry magmatic systems (less than 0.5–1.0 wt% H_2O), stacked sills with incompressible melts form in subsolidus country rocks; melt accumulates near the seismic Moho when magma input rates are low, and in the upper crust when magma input rates are high. By contrast, water-rich arc magmatic systems are typically vertically extensive and dominated by mushy super-solidus conditions except at shallow levels, where compressible gas-rich caps and lenses are common (figure 1). An important but poorly constrained region in all magmatic systems is the magmatic-hydrothermal interface, which is an important location of heat and fluid transfer.

7. Modelling magma reservoir processes

(a) How is a magma reservoir built?

Magma reservoirs may be built, over long timescales, by repeated injections of magma [33,210–212]. Modelling shows that emplacement of basaltic sills into the (amphibolitic) lower crust generates zones of partial melting, with mixing of these anatectic melts with the evolved melts derived from the basalt intrusion. The relative importance of these two components depends on the magma supply rate, but melt differentiation is fundamentally driven by melt migration upward through the partially molten matrix by reactive flow [211] (figure 7). To build a long-lived zone of partial melt in the crust, it is necessary to supply more heat by advection than is lost by conduction [2,33]. Numerical models show that it is easier to form persistent regions of melt-bearing crust (reservoirs) in the (hotter) lower crust than in the cooler upper crust [33]. The magma supply rates should not, however, be sufficiently high to trigger eruptions and thereby prevent magma accumulation. The development of extensive mush regions in the lower crust in the models is consistent with prevailing views of lower crustal fractionation, mixing and assimilation based on magma geochemistry [213]. The inevitable involvement of crustal partial melts in melt differentiation also explains the pervasive crustal signatures observed in the geochemical characteristics of granites and eruptions from large rhyolite bodies [214,215].

It has been suggested that large, upper crustal magma reservoirs may form only if a sufficiently large lower crustal mushy reservoir exists [216]. Such a lower crustal reservoir is likely to be active over timescales of 10^5–10^6 years and may be similar to that imaged beneath Yellowstone caldera [64]. The presence of this lower crustal magma reservoir elevates the upper crustal geotherm sufficiently such that an upper crustal magma reservoir can form with magma fluxes that are 1–2 orders of magnitude lower than for a cold upper crust. Under these conditions, the upper crustal mush can remain stable for 10^5–10^6 years [216], which is in line with the radiometric ages

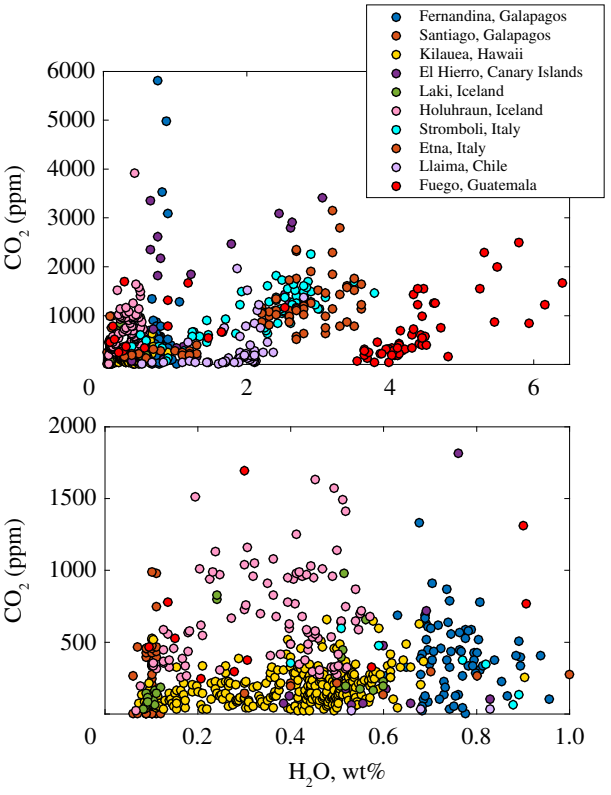

Figure 6. The differences in water contents between arc and hotspot melts may lead to fundamental differences in the form and extent of the magma reservoirs in these settings. Magmatic systems in arc settings will generate larger fractions of exsolved volatiles; and will undergo degassing-induced crystallization at greater depths in the crust [139], which promotes the generation of crystal mushes. Olivine melt inclusion concentrations of H_2O and CO_2, for a range of ocean island volcanic products. The bottom plot is a zoomed in portion of the top plot. Isobars, labelled with pressure in MPa, are shown, appropriate for basalt [199]. Data for Fernandina and Santiago from [200]; for Kīlauea from [54], for El Hierro from [201] for Laki [90], for Holuhraun [86], for Stromboli [202], for Etna [203] for Llaima [204,205] and for Fuego [206–209].

of crystals erupted from large continental magma bodies [162,164]. To generate large eruptible volumes (similar to those erupted by 'supervolcanoes' [217]) requires not only high magma flux, but also protracted magmatic activity [216]. These concepts are likely to prove useful in modelling the formation of hydrothermal ore deposits in crustal environments (figure 7).

(b) Modelling mush recharge, mixing and disaggregation

The evidence discussed in earlier sections suggests that crystal-rich magmas are often disrupted by intruding melts (and perhaps erupted) on timescales of years to decades. How may a locked crystal mush be remobilized on such short timescales? What are the material properties of the mush? How does it deform in response to stress? Numerical models have been developed to answer some of these questions [27,218], based on particle–particle–fluid coupling and interactions at the crystal scale. The results indicate that the mush may become fluidized, with crystals entrained by the intruding melt and efficiently mixed. This and other mixing processes that can occur during ascent and shallower storage (e.g. laminar flow in a shear zone, perhaps in the conduit) may explain the coexistence of antecrysts and phenocrysts that have experienced very different petrogenetic histories [29,133,154].

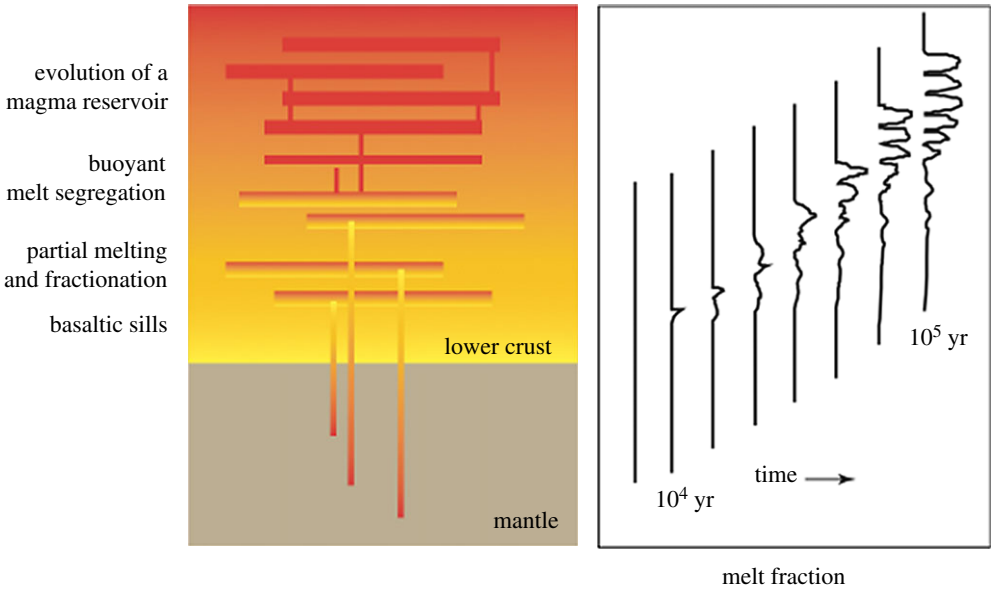

Figure 7. Models have been developed to simulate emplacement of successive sills in the lower amphibolite crust [33,210,211]. The sills crystallize, and heat the surrounding crust, eventually generating melting. The mixed melts (residual melts from the basalts and partial melts of the crust) segregate by buoyant flow along grain boundaries. Over time, repeated injections of basalt leads to upward-migrating permanent melt lenses in the lower crust [211]. There are important implications of such a process: melts differentiate by reactive flow during upward percolation; and there is substantial assimilation of crustal melts.

Magma intrusion into pre-existing, partially solidified sills, can create complex density profiles, as reviewed by Woods & Stock [219]. For example, density-stratified cumulate layers may be interspersed with more homogeneous layers. Crystal-rich suspensions also have complex rheologies. Crystal mush with a touching framework of crystals can support a stress. Intrusion of a liquid-rich magma into the crystal mush, however, may dilate it sufficiently to mobilize the suspension, thereby allowing new melt to intrude [219]. The heterogeneity in crustal architecture produced by successive intrusions then controls the loci of successive intrusions, and the ability of magmas to ascend through the crust [219]. Other factors that may affect the local formation and ascent of magmas include compaction waves and buoyancy layers in the mush (which may be melts or exsolved volatiles) which may be unstable and overturn, reviewed by Sparks *et al.* [2,17]. On longer timescales, magmatic systems may form stably stratified layers as felsic melts ascend to shallow depths, thus creating the structure observed in exposed crustal sections [98].

8. Applications to volcano monitoring

What implications does our new understanding of the depth and form of magma reservoirs have for monitoring (and forecasting) eruptions? The previous sections summarize geophysical and petrological evidence for multiple magma storage areas in the crust, and deep storage regions that are vertically and/or laterally extensive. Magmas fractionate and mix when injected into mushy regions, where they may pick up crystals from a transiently mobilized mush. Magma may be compositionally zoned within a single melt lens as well as throughout the crust, and may comprise mush-dominated, or even subsolidus, over long times. Near-solidus magma reservoirs are remobilized by intruding (more mafic) magmas that may entrain individual crystals, glomerocrysts or cognate xenoliths from the mush, which may then be erupted. Importantly, intrusions of more primitive magma do not always produce eruptions, even when they are

volatile-rich. Instead, exsolved volatiles may accumulate in the upper melt-rich parts of the magma systems, particularly in intermediate and evolved magmatic systems found in subduction zone and continental settings. Migrating volatiles may then trigger instabilities, magma mixing and bursts of outgassing, with or without eruptions. Alternatively, if volatiles are not outgassed, they may contribute to the formation of hydrothermal ore deposits.

How does this heuristic model of magmatic system behaviour help to interpret observations of volcanic behaviour and the signals measured at the surface during periods of unrest and volcanic eruptions? Pritchard *et al*. [220] explore the implications of a *trans-crustal magmatic system* [9] for evaluating signals—seismic, deformation, outgassing—associated with non-magmatic unrest, and those which may be precursors to volcanic eruptions. Generalized models for pre-eruptive seismicity [220,221] include deep (greater than 5 km) Volcano Tectonic (VT) earthquake swarms followed by shallower Long Period events and tremor leading up to eruption; the latter are thought to be associated with the flow of gas-rich magma. These trends are generally consistent with upwards magma transport from the mid-crust prior to eruptions, perhaps triggered within a magma body by pressurization induced by second boiling [26] or by intrusion of deep magma. In detail, however, stress changes can also propagate downwards after the onset of an eruption [222], and demonstrate the importance of pressure changes caused by both conduit development [223] and emptying of shallow magma storage regions; this may happen sequentially when the magmatic system comprises stacked sills [222]. These kinds of trends were also observed after the onset of the 1959 Kīlauea Iki eruption, where deep VT swarms (greater than 30 km) occurred after the onset of the eruption [224]. Critically, a considerable quantity of melt may be stored simultaneously in lenses at different depths in the crust, and perhaps also in the uppermost mantle; this suggests that very large eruptions may not require magma accumulation into a single very large magma chamber, but instead may result from tapping multiple vertically or laterally oriented magma bodies [225–227].

Ground displacements measured by InSAR and well-populated GPS networks are also variable, with inversions varying from simple geometric sources to multiple, complex sources [49,227], often at a range of depths. Additionally, ground displacements are frequently muted, and not as large as expected for the volume of erupted magma. This can be explained by magma compressibility, whereby the presence of an exsolved gas phase allows the magma to contract as pressure increases, diminishing the displacement signal observed at the surface [74,179,180,228]. This compressibility effect has recently been linked directly to gas emissions during explosive eruptions, an analysis which shows that shallower and more water-rich magmas typically show this compressibility signature, and these eruptions are often linked with high gas emissions [181]. Improving interpretations of ground deformation data thus requires a better understanding of the role of the exsolved gas phase in modifying the physical properties of the magma reservoir, reviewed by Segall [73].

Post-eruptive subsidence can be linked to a viscoelastic response associated with a ductile region of melt-bearing crust [229–232]. The deformation consequences of a viscoelastic aureole surrounding a spherical magma chamber can be modelled [73]. This scenario might correspond to the case where magma is intruded and heats the surrounding country rock, or when magma intrudes (or leaves, during explosive eruption) a mushy region of the crust. Interestingly, the post-eruption inflation may occur (without recharge) if the magma is volatile-free or volatile-poor (i.e. incompressible); this result holds for both oblate and prolate geometries. If the magma is sufficiently compressible, post-eruptive deformation will be deflation. These models raise the possibility of reconciling petrological inferences related to pressure changes with observations of deformation. In fact, the timescales derived from diffusion studies described in §5 have been linked directly to the occurrence of earthquake swarms and deformation prior to, and during, eruptions [162,165,233,234]. These correlations show that the monitoring signals are linked to significant pressure and/or temperature perturbations, such as those expected for magma movement and/or mixing in shallow crustal reservoirs.

Gas emissions during and between eruptions also hold a clue to processes occurring in crustal magma reservoirs. Some volcanoes exhibit strong correlations between the mass of

erupted magma and the mass flux of SO_2 (e.g. Kīlauea; [235]), suggesting that degassing occurs in a shallow reservoir and that gas is advected by the magma to the surface, making the SO_2 flux a good proxy for eruption rate. In other settings, however, the patterns of gas emission are rather different. At many volcanoes, an elevated gas flux is maintained between eruptions, e.g. at Bagana, Etna, Stromboli, Colima, Popocatepetl volcanoes [236]. At open-vent basaltic volcanoes, convection of magma in a conduit provides a sustained and steady supply of gas to the atmosphere e.g. at Masaya, Stromboli, Villarica, Nyiragongo, Erta Ale, Ambrym volcanoes [237,238]. Superimposed on this steady supply is the arrival of large CO_2-rich gas slugs and bubbles derived from deeper in the system; this is typical of volcanoes exhibiting strombolian activity such as Stromboli and Yasur volcanoes [239]. Steady-state convection requires deep magma storage bodies for degassed magmas to accumulate, thereby growing the crust endogenously [240]. The formation of gas slugs further requires re-supply of CO_2-rich magma at depth, most probably sourced from gas segregation in sills [241].

At intermediate volcanoes, where magmas undergo significant decompressional degassing and crystallization and where the magmas are more evolved and crystal-rich, gas may accumulate throughout the plumbing system. Gas migration in these systems varies with suspension crystallinity and gas volume; importantly gas migration through crystal-rich mush can be slow, under conditions where bubbles are trapped within the mush [242], or fast, where gas migrates through open, quasi-brittle fractures [185,187]. Sustained, open pathways that allow the passage of deep-derived magmatic gases to the surface have been invoked to explain the high and continuous emission of SO_2 gas at Soufrière Hills Volcano, where it is known that sulfur partitions into an exsolved vapour phase at less than 5–7 km depth [194,243,244]. These pathways may also exist at other volcanoes exhibiting sustained degassing with little eruptive flux.

9. Conclusion and future challenges

(a) Summary and conclusions

— In this volume, we bring together a range of disciplines and types of observations and models to define the state of our understanding of magma reservoirs, and future directions of research. The results of our discussion meeting have highlighted a range of possible directions. It is clear that geophysical methods, combined with petrological barometry, offer a powerful way to delineate the depth of magma bodies, but the information obtained from these methods is not straightforward to reconcile, given the differences in temporal and spatial scales.

— The evidence for magma mixing is ubiquitous in all tectonic settings, and includes mixed and mingled crystals and melts, as well as entrainment of mush components in intruding melts, which may then be erupted at the surface. There are still fundamental questions about whether and when ascending melts may intersect 'foreign' mushes which are not products of their own liquid line of descent. In most cases, it appears that entrained antecrysts are related genetically to the carrier liquids.

— There remains considerable heterogeneity in reservoir architecture from place to place, which ranges from extensive mush-dominated magmatic systems (in the arc crust), to multiple dispersed sills in the country rock (or subsolidus parts of the reservoir) that may contain magma prior to and between eruptions (Iceland).

— The water content of melt exerts an important control on the architecture of magmatic systems. Relatively dry systems appear to be dominated by stacked sills with incompressible melts in subsolidus country rocks; water-rich systems, in contrast, develop vertically extensive mushy super-solidus reservoirs with compressible gas-rich caps and upper crustal lenses.

— Timescales of magmatic processes point to prolonged storage (10^3–10^6 years) in the crust, followed by rapid remobilization and ascent. This remobilization may occur from shallow

storage regions (in evolved systems) or deep sills, perhaps even close to the Moho (in ocean island settings).

— Exsolved volatiles are an important part of the magmatic system, particularly in arc settings. Here, gas-rich regions may form where gas is 'held up' in liquid lenses, but may also be present in the mush and thus may affect its rheological properties. The gas may also generate instabilities in the magmatic system, which may cause local mixing, or even eruption.

— Models describing magma reservoir construction show that important parameters include the magma supply rate (coupled with the accommodation space available) and the thermal state of the crust. Preconditioned upper crust may be most favourable for the formation of large magma reservoirs required to feed supervolcanic eruptions.

— Models of magma emplacement into viscous mush show that complex layering and instabilities may form on crustal scale, owing to the thermal and mechanical effects of intrusion, partial melting, cooling, convection, mixing, degassing and crystal settling. On a particle scale, high input rates of magma recharge into a mush may trigger chaotic mixing and entrainment of crystal cargo.

— Our new understanding of trans-crustal magmatic systems will prove useful for interpretation of volcano monitoring data. Improved seismic networks may show that downward-propagating seismic swarms after the onset of eruptions are common. Such events may even be detected during periods of unrest, which will tell us something about intrusion and instabilities in the magmatic system, particularly when combined with other observations of the volcanic system. Increasingly sophisticated modelling of viscoelasticity means that we can now attempt to explain some of the time-dependent signals that occur after eruptions. Volcanic degassing fluxes (typically SO_2) may be used to infer deep gas accumulation and release processes, particularly for intermediate volcanoes, but also for mafic open vent volcanoes that emit a lot of gas but little magma, requiring gas-melt segregation and the accumulation of large volumes of mushy cumulate magma at depth.

(b) Future challenges

This issue contains new observational constraints on micro-scale textures and compositions of magma components, on thermal conditions of storage and timescales of mobilization from dating and diffusion modelling, and results from a new generation of physical and numerical models which examine processes of heat and mass transfer in crystal mush at the grain scale. These studies offer the potential to make rapid progress in understanding the dynamics of magma reservoirs and the eruptions that they produce. Outstanding questions relate to the mechanisms and timescales of liquid extraction from mush and are summarized below.

— An outstanding question is 'does compaction operate in crustal systems, and if not, what are alternative processes?' How is the physical process of melt extraction modified by reactive flow, production of latent heat and the presence of an MVP?

— How do we detect structures and processes, some at quite small scale, in ductile magmatic environments? What laboratory experiments and advances in theory are needed to constrain the key physical properties and dynamics of magma reservoirs?

— What models need to be developed to understand trans-crustal mush system dynamics, including the magma fluxes, timescales, volumes produced during episodic volcanism? Can these models be coupled to conduit and surface flow models to provide the basis for forecasts? To what extent do we need to re-examine basic assumptions in view of the emerging idea of dynamic mush-magma systems?

— There is substantial work required to better interpret volcano monitoring data. Mass must be conserved during magma transport in the crust, so when we see shallow inflation (as measured by surface ground displacements), we should see deeper deflation. As yet,

however, our measurements are not precise enough. How can we image deeper magma reservoirs? A step change in technology is required.

— The inherent limitations of individual techniques require integration of datasets to better understand magma reservoirs, which calls for sophisticated modelling approaches [245]. Additionally, the growing importance of satellite-based sensors for global monitoring provides exciting opportunities, but also new tools for rapid data processing and integration with models are required.

Data accessibility. This article has no additional data.

Authors' contribution. All authors contributed equally to this manuscript.

Competing interests. The authors declare that they have no competing interests.

Funding. The authors acknowledge the Royal Society for the funding provided to hold the Theo Murphy Royal Society Discussion Meeting at the Kavli Centre in November 2017.

Acknowledgements. NERC COMET are acknowledged for providing support for the meeting.

References

1. Bachmann O, Bergantz GW. 2008 Rhyolites and their source mushes across tectonic settings. *J. Petrol.* **49**, 2277–2285. (doi:10.1093/petrology/egn068)
2. Sparks RSJ, Annen C, Blundy JD, Cashman KV, Rust AC, Jackson MD. 2019 Formation and dynamics of magma reservoirs. *Phil. Trans. R. Soc. A* **377**, 20180019. (doi:10.1098/rsta.2018.0019)
3. Cooper KM, Kent AJ. 2014 Rapid remobilization of magmatic crystals kept in cold storage. *Nature* **506**, 480–483. (doi:10.1038/nature12991)
4. Wager L, Brown G, Wadsworth W. 1960 Types of igneous cumulates. *J. Petrol.* **1**, 73–85. (doi:10.1093/petrology/1.1.73)
5. McKenzie D. 1985 The extraction of magma from the crust and mantle. *Earth Planet. Sci. Lett.* **74**, 81–91. (doi:10.1016/0012-821X(85)90168-2)
6. Bachmann O, Bergantz GW. 2004 On the origin of crystal-poor rhyolites: extracted from batholithic crystal mushes. *J. Petrol.* **45**, 1565–1582. (doi:10.1093/petrology/egh019)
7. Sisson T, Bacon C. 1999 Gas-driven filter pressing in magmas. *Geology* **27**, 613–616. (doi:10.1130/0091-7613(1999)027<0613:GDFPIM>2.3.CO;2)
8. Pistone M *et al.* 2015 Gas-driven filter pressing in magmas: Insights into in-situ melt segregation from crystal mushes. *Geology* **43**, 699–702. (doi:10.1130/g36766.1)
9. Cashman KV, Sparks RSJ, Blundy JD. 2017 Vertically extensive and unstable magmatic systems: a unified view of igneous processes. *Science* **355**, eaag3055. (doi:10.1126/science.aag3055)
10. Marsh BD. 2006 Dynamics of magmatic systems. *Elements* **2**, 287–292. (doi:10.2113/gselements.2.5.287)
11. White RS, Edmonds M, Maclennan J, Greenfield T, Agustsdottir T. 2019 Melt movement through the Icelandic crust. *Phil. Trans. R. Soc. A* **377**, 20180010. (doi:10.1098/rsta.2018.0010)
12. Maclennan J. 2019 Mafic tiers and transient mushes: evidence from Iceland. *Phil. Trans. R. Soc. A* **377**, 20180021. (doi:10.1098/rsta.2018.0021)
13. Maclennan J, McKenzie D, Gronvöld K, Slater L. 2001 Crustal accretion under northern Iceland. *Earth Planet. Sci. Lett.* **191**, 295–310. (doi:10.1016/S0012-821X(01)00420-4)
14. Gudmundsson A. 1995 Infrastructure and mechanics of volcanic systems in Iceland. *J. Volcanol. Geotherm. Res.* **64**, 1–22. (doi:10.1016/0377-0273(95)92782-Q)
15. Korenaga J, Kelemen PB. 1998 Melt migration through the oceanic lower crust: a constraint from melt percolation modeling with finite solid diffusion. *Earth Planet. Sci. Lett.* **156**, 1–11. (doi:10.1016/S0012-821X(98)00004-1)
16. Greenfield T, White RS. 2015 Building Icelandic igneous crust by repeated melt injections. *J. Geophys. Res. Solid Earth* **120**, 7771–7788. (doi:10.1002/2015JB012009)
17. Christopher T, Blundy J, Cashman K, Cole P, Edmonds M, Smith P, Sparks RSJ, Stinton A. 2015 Crustal-scale degassing due to magma system destabilization and magma-gas decoupling at Soufrière Hills Volcano, Montserrat. *Geochem. Geophys. Geosyst.* **16**, 2797–2811. (doi:10.1002/2015gc005791)
18. Lejeune AM, Richet P. 1995 Rheology of crystal-bearing silicate melts: An experimental study at high viscosities. *J. Geophys. Res. Solid Earth* **100**, 4215–4229. (doi:10.1029/94JB02985)

19. Pistone M, Caricchi L, Ulmer P, Reusser E, Ardia P. 2013 Rheology of volatile-bearing crystal mushes: mobilization vs. viscous death. *Chem. Geol.* **345**, 16–39. (doi:10.1016/j.chemgeo.2013.02.007)
20. Pistone M, Caricchi L, Ulmer P, Burlini L, Ardia P, Reusser E, Marone F, Arbaret L. 2012 Deformation experiments of bubble-and crystal-bearing magmas: rheological and microstructural analysis. *J. Geophys. Res. Solid Earth* **117,** B05208. (doi:10.1029/2011jb008986)
21. Caricchi L, Burlini L, Ulmer P, Gerya T, Vassalli M, Papale P. 2007 Non-Newtonian rheology of crystal-bearing magmas and implications for magma ascent dynamics. *Earth Planet. Sci. Lett.* **264**, 402–419. (doi:10.1016/j.epsl.2007.09.032)
22. Huber C, Bachmann O, Dufek J. 2011 Thermo-mechanical reactivation of locked crystal mushes: Melting-induced internal fracturing and assimilation processes in magmas. *Earth Planet. Sci. Lett.* **304**, 443–454. (doi:10.1016/j.epsl.2011.02.022)
23. Guo X, Zhang L, Behrens H, Ni H. 2016 Probing the status of felsic magma reservoirs: constraints from the P–T–H_2O dependences of electrical conductivity of rhyolitic melt. *Earth Planet. Sci. Lett.* **433**, 54–62. (doi:10.1016/j.epsl.2015.10.036)
24. Ruprecht P, Bergantz GW, Dufek J. 2008 Modeling of gas-driven magmatic overturn: tracking of phenocryst dispersal and gathering during magma mixing. *Geochem. Geophys. Geosyst.* **9**, Q07017. (doi:10.1029/2008gc002022)
25. Woods AW, Cowan A. 2009 Magma mixing triggered during volcanic eruptions. *Earth Planet. Sci. Lett.* **288**, 132–137. (doi:10.1016/j.epsl.2009.09.015)
26. Tait S, Jaupart C, Vergniolle S. 1989 Pressure, gas content and eruption periodicity of a shallow, crystallising magma chamber. *Earth Planet. Sci. Lett.* **92**, 107–123. (doi:10.1016/0012-821X(89)90025-3)
27. Bergantz G, Schleicher J, Burgisser A. 2015 Open-system dynamics and mixing in magma mushes. *Nat. Geosci.* **8**, 793–796. (doi:10.1038/ngeo2534)
28. Edmonds M, Aiuppa A, Humphreys M, Moretti R, Giudice G, Martin RS, Herd RA, Christopher T. 2010 Excess volatiles supplied by mingling of mafic magma at an andesite arc volcano. *Geochem. Geophys. Geosyst.* **11**, Q04005. (doi:10.1029/2009gc002781)
29. Ruprecht P, Bachmann O. 2010 Pre-eruptive reheating during magma mixing at Quizapu volcano and the implications for the explosiveness of silicic arc volcanoes. *Geology* **38**, 919–922. (doi:10.1130/G31110.1)
30. Plail M, Edmonds M, Woods AW, Barclay J, Humphreys MC, Herd RA, Christopher T. 2018 Mafic enclaves record syn-eruptive basalt intrusion and mixing. *Earth Planet. Sci. Lett.* **484**, 30–40. (doi:10.1016/j.epsl.2017.11.033)
31. Linde AT, Sacks IS. 1998 Triggering of volcanic eruptions. *Nature* **395**, 888. (doi:10.1038/27650)
32. Crisp JA. 1984 Rates of magma emplacement and volcanic output. *J. Volcanol. Geotherm. Res.* **20**, 177–211. (doi:10.1016/0377-0273(84)90039-8)
33. Annen C, Blundy JD, Leuthold J, Sparks RSJ. 2015 Construction and evolution of igneous bodies: Towards an integrated perspective of crustal magmatism. *Lithos* **230**, 206–221. (doi:10.1016/j.lithos.2015.05.008)
34. Bachmann O, Cd M, De Silva S. 2007 The volcanic–plutonic connection as a stage for understanding crustal magmatism. *J. Volcanol. Geotherm. Res.* **167**, 1–23. (doi:10.1016/j.jvolgeores.2007.08.002)
35. Huppert HE, Sparks R. 1988 The generation of granitic magmas by intrusion of basalt into continental crust. *J. Petrol.* **29**, 599–624. (doi:10.1093/petrology/29.3.599)
36. Paterson SR, Ardill K, Vernon R, Žák J. 2018 A review of mesoscopic magmatic structures and their potential for evaluating the hypersolidus evolution of intrusive complexes. *J. Struct. Geol.* (doi:10.1016/j.jsg.2018.04.022)
37. Glazner AF, Coleman DS, Mills RD. 2018 The volcanic-plutonic connection. In *Physical geology of shallow magmatic systems*, (eds C Breitkreuz, S Rocchi), pp. 61–82. Berlin, Germany: Springer.
38. Lowenstern JB, Sisson TW, Hurwitz S. 2017 Probing magma reservoirs to improve volcano forecasts. *EOS-Earth Space Sci. News* **98**. (doi:10.1029/2017eo085189)
39. Neave DA, Passmore E, Maclennan J, Fitton G, Thordarson T. 2013 Crystal–melt relationships and the record of deep mixing and crystallization in the ad 1783 Laki Eruption, Iceland. *J. Petrol.* **54**, 1661–1690. (doi:10.1093/petrology/egt027)

40. Paterson S, Schmidt K. 1999 Is there a close spatial relationship between faults and plutons? *J. Struct. Geol.* **21**, 1131–1142. (doi:10.1016/S0191-8141(99)00024-3)
41. Hutton DH. 1988 Granite emplacement mechanisms and tectonic controls: inferences from deformation studies. *Earth Environ. Sci. Trans. R. Soc. Edinb.* **79**, 245–255. (doi:10.1017/S0263593300014255)
42. Emeleus C, Cheadle M, Hunter R, Upton B, Wadsworth W. 1996 The Rum layered suite. In *Developments in petrology*, vol. 15, (ed. RG Cawthorn), pp. 403–439. Amsterdam, The Netherlands: Elsevier.
43. John BE, Blundy JD. 1993 Emplacement-related deformation of granitoid magmas, southern Adamello Massif, Italy. *Geol. Soc. Am. Bull.* **105**, 1517–1541. (doi:10.1130/0016-7606(1993)105<1517:ERDOGM>2.3.CO;2)
44. Feuillet N *et al.* 2010 Active faulting induced by slip partitioning in Montserrat and link with volcanic activity: New insights from the 2009 GWADASEIS marine cruise data. *Geophys. Res. Lett.* **37**. (doi:10.1029/2010gl042556)
45. Fink JH. 1985 Geometry of silicic dikes beneath the Inyo Domes, *California*. *J. Geophys. Res. Solid Earth* **90**, 11 127–11 133. (doi:10.1029/JB090iB13p11127)
46. Pasquaré F, Tibaldi A. 2003 Do transcurrent faults guide volcano growth? The case of NW Bicol Volcanic Arc, Luzon, Philippines. *Terra Nova.* **15**, 204–212. (doi:10.1046/j.1365-3121.2003.00484.x)
47. Wright TJ, Ebinger C, Biggs J, Ayele A, Yirgu G, Keir D, Stork A. 2006 Magma-maintained rift segmentation at continental rupture in the 2005 Afar dyking episode. *Nature* **442**, 291–294. (doi:10.1038/nature04978)
48. Hutchison W, Mather TA, Pyle DM, Biggs J, Yirgu G. 2015 Structural controls on fluid pathways in an active rift system: a case study of the Aluto volcanic complex. *Geosphere* **11**, 542–562. (doi:10.1130/GES01119.1)
49. Biggs J, Annen C. 2018 The lateral growth and coalesence of magma systems. *Phil. Trans. R. Soc. A* **376**, 20180005. (doi:10.1098/rsta.2018.0005)
50. Darbyshire FA, White RS, Priestley KF. 2000 Structure of the crust and uppermost mantle of Iceland from a combined seismic and gravity study. *Earth Planet. Sci. Lett.* **181**, 409–428. (doi:10.1016/S0012-821X(00)00206-5)
51. Hudson T, White RS, Greenfield T, Ágústsdóttir T, Brisbourne A, Green RG. 2017 Deep crustal melt plumbing of Bárðarbunga volcano, Iceland. *Geophys. Res. Lett.* **44**, 8785–8794. (doi:10.1002/2017GL074749)
52. Gudmundsson MT *et al.* 2016 Gradual caldera collapse at Bárdarbunga volcano, Iceland, regulated by lateral magma outflow. *Science* **353**, aaf8988. (doi:10.1126/science.aaf8988)
53. Ágústsdóttir T, Woods J, Greenfield T, Green RG, White RS, Winder T, Brandsdóttir B, Steinthórsson S, Soosalu H. 2016 Strike-slip faulting during the 2014 Bárðarbunga-Holuhraun dike intrusion, central Iceland. *Geophys. Res. Lett.* **43**, 1495–1503. (doi:10.1002/2015GL067423)
54. Sides IR, Edmonds M, Maclennan J, Swanson DA, Houghton BF. 2014 Eruption style at Kīlauea Volcano in Hawaìi linked to primary melt composition. *Nat. Geosci.* **7**, 464–469. (doi:10.1038/ngeo2140)
55. Helz RL, Clague DA, Sisson TW, Thornber CR. 2014 Petrologic insights into basaltic volcanism at historically active Hawaiian volcanoes: Chapter 6 in Characteristics of Hawaiian volcanoes. *US Geological Survey* 2330–7102.
56. Bagnardi M, Amelung F. 2012 Space-geodetic evidence for multiple magma reservoirs and subvolcanic lateral intrusions at Fernandina Volcano, Galápagos Islands. *J. Geophys. Res. Solid Earth* **117**, B10406. (doi:10.1029/2012jb009465)
57. Ebmeier S *et al.* 2018 Synthesis of global satellite observations of magmatic and volcanic deformation: implications for volcano monitoring & the lateral extent of magmatic domains. *J. Appl. Volcanol.* **7**, 2. (doi:10.1186/s13617-018-0071-3)
58. White RS, Drew J, Martens HR, Key J, Soosalu H, Jakobsdóttir SS. 2011 Dynamics of dyke intrusion in the mid-crust of Iceland. *Earth Planet. Sci. Lett.* **304**, 300–312. (doi:10.1016/j.epsl.2011.02.038)
59. Soosalu H, Key J, White RS, Knox C, Einarsson P, Jakobsdóttir SS. 2010 Lower-crustal earthquakes caused by magma movement beneath Askja volcano on the north Iceland rift. *Bull. Volcanol.* **72**, 55. (doi:10.1007/s00445-009-0297-3)

60. Martens HR, White RS. 2013 Triggering of microearthquakes in Iceland by volatiles released from a dyke intrusion. *Geophys. J. Int.* **194**, 1738–1754. (doi:10.1093/gji/ggt184)
61. Shelly DR, Hill DP. 2011 Migrating swarms of brittle-failure earthquakes in the lower crust beneath Mammoth Mountain, California. *Geophys. Res. Lett.* **38**, L20307.
62. Kiser E, Levander A, Zelt C, Schmandt B, Hansen S. 2018 Focusing of melt near the top of the Mount St. Helens (USA) magma reservoir and its relationship to major volcanic eruptions. *Geology* **46**, 775–778. (doi:10.1130/G45140.1)
63. Vargas CA, Koulakov I, Jaupart C, Gladkov V, Gomez E, El Khrepy S, Al-Arifi N. 2017 Breathing of the Nevado del Ruiz volcano reservoir, Colombia, inferred from repeated seismic tomography. *Sci. Rep.* **7**, 46094. (doi:10.1038/srep46094)
64. Farrell J, Smith RB, Husen S, Diehl T. 2014 Tomography from 26 years of seismicity revealing that the spatial extent of the Yellowstone crustal magma reservoir extends well beyond the Yellowstone caldera. *Geophys. Res. Lett.* **41**, 3068–3073. (doi:10.1002/2014GL059588)
65. Huang H-H, Lin F-C, Schmandt B, Farrell J, Smith RB, Tsai VC. 2015 The Yellowstone magmatic system from the mantle plume to the upper crust. *Science* **348**, 773–776. (doi:10.1126/science.aaa5648)
66. Magee C *et al.* 2018 Magma plumbing systems: a geophysical perspective. *J. Petrol.* **59**, 1217–1251. (doi:10.1093/petrology/egy064)
67. Comeau MJ, Unsworth MJ, Cordell D. 2016 New constraints on the magma distribution and composition beneath Volcán Uturuncu and the southern Bolivian Altiplano from magnetotelluric data. *Geosphere* **12**, 1391–1421. (doi:10.1130/GES01277.1)
68. Hübert J, Whaler K, Fisseha S. 2018 The electrical structure of the central main Ethiopian Rift as imaged by magnetotellurics: implications for magma storage and pathways. *J. Geophys. Res. Solid Earth* **123**, 6019–6032. (doi:10.1029/2017JB015160)
69. Laumonier M, Gaillard F, Muir D, Blundy J, Unsworth M. 2017 Giant magmatic water reservoirs at mid-crustal depth inferred from electrical conductivity and the growth of the continental crust. *Earth Planet. Sci. Lett.* **457**, 173–180. (doi:10.1016/j.epsl.2016.10.023)
70. Bedrosian PA, Peacock JR, Bowles-Martinez E, Schultz A, Hill GJ. 2018 Crustal inheritance and a top-down control on arc magmatism at Mount St. Helens. *Nat. Geosci.* **11**, 865–870. (doi:10.1038/s41561-018-0217-2)
71. Desissa M, Johnson N, Whaler K, Hautot S, Fisseha S, Dawes G. 2013 A mantle magma reservoir beneath an incipient mid-ocean ridge in Afar, Ethiopia. *Nat. Geosci.* **6**, 861–865. (doi:10.1038/ngeo1925)
72. Walter T, Shirzaei M, Manconi A, Solaro G, Pepe A, Manzo M, Sansosti E. 2014 Possible coupling of Campi Flegrei and Vesuvius as revealed by InSAR time series, correlation analysis and time dependent modeling. *J. Volcanol. Geotherm. Res.* **280**, 104–110. (doi:10.1016/j.jvolgeores.2014.05.006)
73. Segall P. 2019 Magma chambers: what we can, and cannot, learn from volcano geodesy. *Phil. Trans. R. Soc. A* **377**, 20180158. (doi:10.1098/rsta.2018.0158)
74. Segall P. 2010 *Earthquake and volcano deformation*. Princeton, NJ: Princeton University Press.
75. Segall P. 2013 Volcano deformation and eruption forecasting. *Geol. Soc. Lond. Spec. Publ.* **380**, 85–106. (doi:10.1144/SP380.4)
76. Biggs J, Pritchard ME. 2017 Global volcano monitoring: what does it mean when volcanoes deform? *Elements* **13**, 17–22. (doi:10.2113/gselements.13.1.17)
77. Biggs J, Amelung F, Gourmelen N, Dixon TH, Kim S-W. 2009 InSAR observations of 2007 Tanzania rifting episode reveal mixed fault and dyke extension in an immature continental rift. *Geophys. J. Int.* **179**, 549–558. (doi:10.1111/j.1365-246X.2009.04262.x)
78. Biggs J, Ebmeier S, Aspinall W, Lu Z, Pritchard M, Sparks R, Mather TA. 2014 Global link between deformation and volcanic eruption quantified by satellite imagery. *Nat. Commun.* **5**, 3471. (doi:10.1038/ncomms4471)
79. Jay J, Costa F, Pritchard M, Lara L, Singer B, Herrin J. 2014 Locating magma reservoirs using InSAR and petrology before and during the 2011–2012 Cordón Caulle silicic eruption. *Earth Planet. Sci. Lett.* **395**:254–266. (doi:10.1016/j.epsl.2014.03.046)
80. Bagnardi M, Amelung F, Poland MP. 2013 A new model for the growth of basaltic shields based on deformation of Fernandina volcano, Galápagos Islands. *Earth Planet. Sci. Lett.* **377**, 358–366. (doi:10.1016/j.epsl.2013.07.016)

81. Mogi K. 1958 Relations between the eruptions of various volcanoes and the deformations of the ground surfaces around them. *Bull. Earthquake Res. Inst. Univ. Tokyo*, **36**, 99–134.
82. Amoruso A, Crescentini L. 2009 Shape and volume change of pressurized ellipsoidal cavities from deformation and seismic data. *J. Geophys. Res. Solid Earth* **114**, B02210. (doi:10.1029/2008jb005946)
83. Lu Z, Dzurisin D. 2010 Ground surface deformation patterns, magma supply, and magma storage at Okmok volcano, Alaska, from InSAR analysis: 2. Coeruptive deflation, July–August 2008. *J. Geophys. Res. Solid Earth* **115**, B00B03. (doi:10.1029/2009jb006970)
84. Wicks C, Yarai H, Lu Z, Helz R 2005 ENVISAT SAR and InSAR observations of deformation and crater floor elevation change of Anatahan Volcano, Mariana Islands. In *AGU Fall Meeting Abstracts*.
85. Yang H-J, Kinzler RJ, Grove T. 1996 Experiments and models of anhydrous, basaltic olivine-plagioclase-augite saturated melts from 0.001 to 10 kbar. *Contr. Mineral Petrol.* **124**, 1–18. (doi:10.1007/s004100050169)
86. Bali E, Hartley M, Halldórsson S, Gudfinnsson G, Jakobsson S. 2018 Melt inclusion constraints on volatile systematics and degassing history of the 2014–2015 Holuhraun eruption, Iceland. *Contr. Mineral Petrol.* **173**, 9. (doi:10.1007/s00410-017-1434-1)
87. Hansteen TH, Klügel A, Schmincke H-U. 1998 Multi-stage magma ascent beneath the Canary Islands: evidence from fluid inclusions. *Contr. Mineral Petrol.* **132**, 48–64. (doi:10.1007/s004100050404)
88. Neave DA, Putirka KD. 2017 A new clinopyroxene-liquid barometer, and implications for magma storage pressures under Icelandic rift zones. *Am. Mineral.* **102**, 777–794. (doi:10.2138/am-2017-5968)
89. Putirka K, Johnson M, Kinzler R, Longhi J, Walker D. 1996 Thermobarometry of mafic igneous rocks based on clinopyroxene-liquid equilibria, 0–30 kbar. *Contr. Mineral Petrol.* **123**, 92–108. (doi:10.1007/s004100050145)
90. Hartley ME, Maclennan J, Edmonds M, Thordarson T. 2014 Reconstructing the deep CO_2 degassing behaviour of large basaltic fissure eruptions. *Earth Planet. Sci. Lett.* **393**, 120–131. (doi:10.1016/j.epsl.2014.02.031)
91. Neave DA, Maclennan J, Edmonds M, Thordarson T. 2014 Melt mixing causes negative correlation of trace element enrichment and CO_2 content prior to an Icelandic eruption. *Earth Planet. Sci. Lett.* **400**, 272–283. (doi:10.1016/j.epsl.2014.05.050)
92. Winpenny B, Maclennan J. 2011 A partial record of mixing of mantle melts preserved in Icelandic phenocrysts. *J. Petrol.* **52**, 1791–1812. (doi:10.1093/petrology/egr031)
93. Hartley ME, Thordarson T. 2013 The 1874–1876 volcano-tectonic episode at Askja, North Iceland: lateral flow revisited. *Geochem. Geophys. Geosyst.* **14**, 2286–309. (doi:10.1002/ggge.20151)
94. Neave DA, Maclennan J, Thordarson T, Hartley ME. 2015 The evolution and storage of primitive melts in the Eastern Volcanic Zone of Iceland: the 10 ka Grímsvötn tephra series (ie the Saksunarvatn ash). *Contr. Mineral Petrol.* **170**, 21. (doi:10.1007/s00410-015-1170-3)
95. Halldorsson SA, Oskarsson N, Gronvold K, Sigurdsson G, Sverrisdottir G, Steinthorsson S. 2008 Isotopic-heterogeneity of the Thjorsa lava—implications for mantle sources and crustal processes within the Eastern Rift Zone, Iceland. *Chem. Geol.* **255**, 305–316. (doi:10.1016/j.chemgeo.2008.06.050)
96. Kelemen PB, Koga K, Shimizu N. 1997 Geochemistry of gabbro sills in the crust-mantle transition zone of the Oman ophiolite: implications for the origin of the oceanic lower crust. *Earth Planet. Sci. Lett.* **146**, 475–488. (doi:10.1016/S0012-821X(96)00235-X)
97. Brandsdóttir B, Menke W, Einarsson P, White RS, Staples RK. 1997 Färoe-Iceland ridge experiment 2. Crustal structure of the Krafla central volcano. *J. Geophys. Res. Solid Earth* **102**, 7867–7886. (doi:10.1029/96JB03799)
98. DeBari SM, Greene AR. 2011 Vertical stratification of composition, density, and inferred magmatic processes in exposed arc crustal sections. In *Arc-continent collision*, (eds D Brown, PD Ryan), pp. 121–144. Berlin, Germany: Springer.
99. Shillington DJ, Van Avendonk HJ, Holbrook WS, Kelemen PB, Hornbach MJ. 2004 Composition and structure of the central Aleutian island arc from arc-parallel wide-angle seismic data. *Geochem. Geophys. Geosyst.* **5**. (doi:10.1029/2004gc000715)

100. Nakanishi A *et al.* 2009 Crustal evolution of the southwestern Kuril Arc, Hokkaido Japan, deduced from seismic velocity and geochemical structure. *Tectonophysics* **472**, 105–123. (doi:10.1016/j.tecto.2008.03.003)
101. Parsons T *et al.* 1998 A new view into the Cascadia subduction zone and volcanic arc: implications for earthquake hazards along the Washington margin. *Geology* **26**, 199–202. (doi:10.1130/0091-7613(1998)026<0199:ANVITC>2.3.CO;2)
102. Suyehiro K *et al.* 1996 Continental crust, crustal underplating, and low-Q upper mantle beneath an oceanic island arc. *Science* **272**, 390–392. (doi:10.1126/science.272.5260.390)
103. Plafker G, Nokleberg W, Lull J. 1989 Bedrock geology and tectonic evolution of the Wrangellia, Peninsular, and Chugach terranes along the Trans-Alaska Crustal Transect in the Chugach Mountains and southern Copper River Basin, Alaska. *J. Geophys. Res. Solid Earth* **94**, 4255–4295. (doi:10.1029/JB094iB04p04255)
104. Hacker BR, Mehl L, Kelemen PB, Rioux M, Behn MD, Luffi P. 2008 Reconstruction of the Talkeetna intraoceanic arc of Alaska through thermobarometry. *J. Geophys. Res. Solid Earth* **113**, B03204. (doi:10.1029/2007jb005208)
105. Treloar PJ, Petterson MG, Jan MQ, Sullivan M. 1996 A re-evaluation of the stratigraphy and evolution of the Kohistan arc sequence, Pakistan Himalaya: implications for magmatic and tectonic arc-building processes. *J. Geol. Soc.* **153**, 681–693. (doi:10.1144/gsjgs.153.5.0681)
106. Burg J, Bodinier J, Chaudhry S, Hussain S, Dawood H. 1998 Infra-arc mantle-crust transition and intra-arc mantle diapirs in the Kohistan Complex (Pakistani Himalaya): petro-structural evidence. *Terra Nova-Oxford.* **10**, 74–80. (doi:10.1046/j.1365-3121.1998.00170.x)
107. Jagoutz O, Schmidt MW. 2012 The formation and bulk composition of modern juvenile continental crust: the Kohistan arc. *Chem. Geol.* **298**, 79–96. (doi:10.1016/j.chemgeo.2011.10.022)
108. Otamendi JE, Ducea MN, Tibaldi AM, Bergantz GW, de la Rosa JD,Vujovich GI. 2009 Generation of tonalitic and dioritic magmas by coupled partial melting of gabbroic and metasedimentary rocks within the deep crust of the Famatinian magmatic arc, Argentina. *J. Petrol.* **50**, 841–873. (doi:10.1093/petrology/egp022)
109. Behn MD, Kelemen PB. 2006 Stability of arc lower crust: Insights from the Talkeetna arc section, south central Alaska, and the seismic structure of modern arcs. *J. Geophys. Res. Solid Earth* **111**, B11207. (doi:10.1029/2006jb004327)
110. Christensen NI, Mooney WD. 1995 Seismic velocity structure and composition of the continental crust: a global view. *J. Geophys. Res. Solid Earth* **100**, 9761–9788. (doi:10.1029/95JB00259)
111. Iwasaki T *et al.* 2001 Extensional structure in northern Honshu Arc as inferred from seismic refraction/wide-angle reflection profiling. *Geophys. Res. Lett.* **28**, 2329–2332. (doi:10.1029/2000GL012783)
112. Marsh BD. 1989 Magma chambers. *Annu. Rev. Earth Planet. Sci.* **17**, 439–472. (doi:10.1146/annurev.ea.17.050189.002255)
113. Mangan MT, Marsh BD. 1992 Solidification front fractionation in phenocryst-free sheet-like magma bodies. *J. Geol.* **100**, 605–620. (doi:10.1086/629611)
114. Naslund H, McBirney A. 1996 Mechanisms of formation of igneous layering. In *Developments in petrology*, **vol. 15**, pp. 1–43. Amsterdam, The Netherlands: Elsevier.
115. Vukmanovic Z, Holness MB, Monks K, Andersen J. 2018 The Skaergaard trough layering: sedimentation in a convecting magma chamber. *Contr. Mineral Petrol.* **173**, 1–18. (doi:10.1007/s00410-018-1466-1)
116. Holness MB, Nielsen TF, Tegner C. 2017 The Skaergaard intrusion of East Greenland: paradigms, problems and new perspectives. Elements: an international magazine of mineralogy. *Geochem. Petrol.* **13**, 391–396.
117. Holness MB, Tegner C, Nielsen TF, Stripp G, Morse SA. 2007 A textural record of solidification and cooling in the Skaergaard intrusion, East Greenland. *J. Petrol.* **48**, 2359–2377. (doi:10.1093/petrology/egm064)
118. Tegner C, Thy P, Holness MB, Jakobsen JK, Lesher CE. 2009 Differentiation and compaction in the Skaergaard intrusion. *J. Petrol.* **50**, 813–840. (doi:10.1093/petrology/egp020)
119. Holness M. 2007 Textural immaturity of cumulates as an indicator of magma chamber processes: infiltration and crystal accumulation in the Rum Eastern Layered Intrusion. *J. Geol. Soc.* **164**, 529–539. (doi:10.1144/0016-76492006-021)

120. Rudge JF, Holness MB, Smith GC. 2008 Quantitative textural analysis of packings of elongate crystals. *Contr Mineral Petrol.* **156**, 413–429. (doi:10.1007/s00410-008-0293-1)
121. Holness MB, Vukmanovic Z, Mariani E. 2017 Assessing the role of compaction in the formation of adcumulates: a microstructural perspective. *J. Petrol.* **58**, 643–673. (doi:10.1093/petrology/egx037)
122. Holness MB, Farr R, Neufeld JA. 2017 Crystal settling and convection in the Shiant Isles Main Sill. *Contr. Mineral Petrol.* **172**, 7. (doi:10.1007/s00410-016-1325-x)
123. Nakamura M. 1995 Continuous mixing of crystal mush and replenished magma in the ongoing Unzen eruption. *Geology* **23**, 807–810. (doi:10.1130/0091-7613(1995)023<0807:CMOCMA>2.3.CO;2)
124. Nakagawa M, Wada K, Wood CP. 2002 Mixed magmas, mush chambers and eruption triggers: evidence from zoned clinopyroxene phenocrysts in andesitic scoria from the 1995 eruptions of Ruapehu volcano, New Zealand. *J. Petrol.* **43**, 2279–2303. (doi:10.1093/petrology/43.12.2279)
125. Huber C, Bachmann O, Manga M. 2010 Two competing effects of volatiles on heat transfer in crystal-rich magmas: thermal insulation vs defrosting. *J. Petrol.* **51**, 847–867. (doi:10.1093/petrology/egq003)
126. Bachmann O, Bergantz GW. 2006 Gas percolation in upper-crustal silicic crystal mushes as a mechanism for upward heat advection and rejuvenation of near-solidus magma bodies. *J. Volcanol. Geotherm. Res.* **149**, 85–102. (doi:10.1016/j.jvolgeores.2005.06.002)
127. Holness MB, Stock MJ, Geist D. 2019 Magma chambers vs mush zones: constraining the architecture of sub-volcanic plumbing systems from microstructural analysis of crystalline enclaves. *Phil. Trans. R. Soc. A* **377**, 20180006. (doi:10.98/rsta.2018.0006)
128. Holness MB, Cesare B, Sawyer EW. 2011 Melted rocks under the microscope: microstructures and their interpretation. *Elements* **7**, 247–252. (doi:10.2113/gselements.7.4.247)
129. Holness MB. 2014 The effect of crystallization time on plagioclase grain shape in dolerites. *Contr. Mineral Petrol.* **168**, 1076. (doi:10.1007/s00410-014-1076-5)
130. Holness MB, Cheadle MJ, McKENZIE D. 2005 On the use of changes in dihedral angle to decode late-stage textural evolution in cumulates. *J. Petrol.* **46**, 1565–1583. (doi:10.1093/petrology/egi026)
131. Holness MB, Humphreys MC, Sides R, Helz RT, Tegner C. 2012 Toward an understanding of disequilibrium dihedral angles in mafic rocks. *J. Geophys. Res. Solid Earth* **117**, B06207. (doi:10.1029/2011jb008902)
132. Humphreys M, Edmonds M, Christopher T, Hards V. 2010 Magma hybridisation and diffusive exchange recorded in heterogeneous glasses from Soufrière Hills Volcano, Montserrat. *Geophys. Res. Lett.* **37**, L00E06. (doi:10.1029/2009GL041926)
133. Humphreys MC, Christopher T, Hards V. 2009 Microlite transfer by disaggregation of mafic inclusions following magma mixing at Soufrière Hills volcano, Montserrat. *Contr. Mineral Petrol.* **157**, 609–624. (doi:10.1007/s00410-008-0356-3)
134. Jerram DA, Cheadle MJ, Philpotts AR. 2003 Quantifying the building blocks of igneous rocks: are clustered crystal frameworks the foundation? *J. Petrol.* **44**, 2033–2051. (doi:10.1093/petrology/egg069)
135. Hammer JE, Sharp TG, Wessel P. 2010 Heterogeneous nucleation and epitaxial crystal growth of magmatic minerals. *Geology* **38**, 367–370. (doi:10.1130/G30601.1)
136. Schwindinger, Anderson. 1985
137. McIntire MZ, Bergantz GW, Schleicher JM. 2019 On the hydrodynamics of crystal clustering. *Phil. Trans. R. Soc. A* **377**, 20180015. (doi:10.1098/rsta.2018.0015)
138. Humphreys MCS, Zhang J, Cooper GF, Macpherson CG, Ottley CJ. 2019 Identifying the ingredients of hydrous arc magmas: insights from Mt Lamington, Papua New Guinea. *Phil. Trans. R. Soc. A* **377**, 20180018. (doi:10.1098/rsta.2018.0018)
139. Cashman KV, Edmonds M. 2019 Mafic glass compositions: a record of magma storage conditions, mixing and ascent. *Phil. Trans. R. Soc. A* **377**, 20180004. (doi:10.1098/rsta.2018.0004)
140. Mangan MT. 1990 Crystal size distribution systematics and the determination of magma storage times: the 1959 eruption of Kilauea volcano, Hawaii. *J. Volcanol. Geotherm. Res.* **44**, 295–302. (doi:10.1016/0377-0273(90)90023-9)

141. Sakyi PA, Tanaka R, Kobayashi K, Nakamura E. 2012 Inherited Pb isotopic records in olivine antecryst-hosted melt inclusions from Hawaiian lavas. *Geochim. Cosmochim. Acta* **95**, 169–195. (doi:10.1016/j.gca.2012.07.025)
142. Deering C, Bachmann O. 2010 Trace element indicators of crystal accumulation in silicic igneous rocks. *Earth Planet. Sci. Lett.* **297**, 324–331. (doi:10.1016/j.epsl.2010.06.034)
143. Stelten ME, Cooper KM. 2012 Constraints on the nature of the subvolcanic reservoir at South Sister volcano, Oregon from U-series dating combined with sub-crystal trace-element analysis of plagioclase and zircon. *Earth Planet. Sci. Lett.* **313**, 1–11. (doi:10.1016/j.epsl.2011.10.035)
144. Clague DA, Denlinger RP. 1994 Role of olivine cumulates in destabilizing the flanks of Hawaiian volcanoes. *Bull. Volcanol.* **56**, 425–434. (doi:10.1007/BF00302824)
145. Maclennan J, McKenzie D, Hilton F, Gronvöld K, Shimizu N. 2003 Geochemical variability in a single flow from northern Iceland. *J. Geophys. Res. Solid Earth* **108**, ECV4-1–ECV4-21. (doi:10.1029/2000jb000142)
146. Kent AJR. 2008 Melt inclusions in basaltic and related volcanic rocks. *Rev. Mineral. Geochem.* **69**, 273–331. (doi:10.2138/rmg.2008.69.8)
147. Storm S, Shane P, Schmitt AK, Lindsay JM. 2011 Contrasting punctuated zircon growth in two syn-erupted rhyolite magmas from Tarawera volcano: insights to crystal diversity in magmatic systems. *Earth Planet. Sci. Lett.* **301**, 511–520. (doi:10.1016/j.epsl.2010.11.034)
148. Cassidy M, Edmonds M, Watt SF, Palmer MR, Gernon TM. 2015 Origin of basalts by hybridization in andesite-dominated arcs. *J. Petrol.* **56**, 325–346. (doi:10.1093/petrology/(egv002))
149. Ruprecht P, Bergantz GW, Cooper KM, Hildreth W. 2012 The crustal magma storage system of Volcán Quizapu, Chile, and the effects of magma mixing on magma diversity. *J. Petrol.* **53**, 801–840. (doi:10.1093/petrology/egs002)
150. Humphreys MC, Blundy JD, Sparks RSJ. 2006 Magma evolution and open-system processes at Shiveluch Volcano: insights from phenocryst zoning. *J. Petrol.* **47**, 2303–2334. (doi:10.1093/petrology/egl045)
151. Humphreys M, Edmonds M, Plail M, Barclay J, Parkes D, Christopher T. 2013 A new method to quantify the real supply of mafic components to a hybrid andesite. *Contr. Mineral Petrol.* **165**, 191–215. (doi:10.1007/s00410-012-0805-x)
152. Murphy M, Sparks R, Barclay J, Carroll M, Brewer T. 2000 Remobilization of andesite magma by intrusion of mafic magma at the Soufriere Hills Volcano, Montserrat, West Indies. *J. Petrol.* **41**, 21–42. (doi:10.1093/petrology/41.1.21)
153. Kent AJ. 2014 Preferential eruption of andesitic magmas: implications for volcanic magma fluxes at convergent margins. *Geol. Soc. Lond. Spec. Publ.* **385**, 257–280. (doi:10.1144/SP385.10)
154. Cashman K, Blundy J. 2013 Petrological cannibalism: the chemical and textural consequences of incremental magma body growth. *Contr. Mineral Petrol.* **166**, 703–729. (doi:10.1007/s00410-013-0895-0)
155. Davidson J, Turner S, Handley H, Macpherson C, Dosseto A. 2007 Amphibole 'sponge' in arc crust? *Geology* **35**, 787–790. (doi:10.1130/G23637A.1)
156. Sinton JM, Detrick RS. 1992 Mid-ocean ridge magma chambers. *J. Geophys. Res. Solid Earth* **97**, 197–216. (doi:10.1029/91JB02508)
157. Langmuir CH, Klein EM, Plank T. 1992 Petrological systematics of mid-ocean ridge basalts: Constraints on melt generation beneath ocean ridges. *Mantle Flow Melt Gen. Mid-Ocean Ridges* **71**, 183–280.
158. McKenzie D, Bickle M. 1988 The volume and composition of melt generated by extension of the lithosphere. *J. Petrol.* **29**, 625–679. (doi:10.1093/petrology/29.3.625)
159. Lissenberg CJ, MacLeod CJ, Bennett EN. 2019 Consequences of a crystal mush-dominated magma plumbing system: a mid-ocean ridge perspective. *Phil. Trans. R. Soc. A* **377**, 20180014. (doi:10.1098/rsta.2018.0014)
160. Lissenberg CJ, MacLeod CJ, Howard KA, Godard M. 2013 Pervasive reactive melt migration through fast-spreading lower oceanic crust (Hess Deep, equatorial Pacific Ocean). *Earth Planet. Sci. Lett.* **361**, 436–447. (doi:10.1016/j.epsl.2012.11.012)
161. Boudier F, Nicolas A, Ildefonse B. 1996 Magma chambers in the Oman ophiolite: fed from the top and the bottom. *Earth Planet. Sci. Lett.* **144**, 239–250. (doi:10.1016/0012-821X(96)00167-7)

162. Cooper KM. 2019 Time scales and temperatures of crystal storage in magma reservoirs: implications for magma reservoir dynamics. *Phil. Trans. R. Soc. A* **377**, 20180009. (doi:10.1098/rsta.2018.0009)
163. Morgan DJ, Blake S. 2006 Magmatic residence times of zoned phenocrysts: introduction and application of the binary element diffusion modelling (BEDM) technique. *Contr. Mineral Petrol.* **151**, 58–70. (doi:10.1007/s00410-005-0045-4)
164. Hawkesworth C, Blake S, Evans P, Hughes R, Macdonald R, Thomas L, Turner SP, Zellmer G. 2000 Time scales of crystal fractionation in magma chambers—integrating physical, isotopic and geochemical perspectives. *J. Petrol.* **41**, 991–1006. (doi:10.1093/petrology/41.7.991)
165. Kahl M, Chakraborty S, Costa F, Pompilio M, Liuzzo M, Viccaro M. 2013 Compositionally zoned crystals and real-time degassing data reveal changes in magma transfer dynamics during the 2006 summit eruptive episodes of Mt. Etna. *Bull. Volcanol.* **75**, 1–14. (doi:10.1007/s00445-013-0692-7)
166. Costa F, Morgan D. 2011 Time constraints from chemical equilibration in magmatic crystals. In *Timescales of magmatic processes: from core to atmosphere*, (eds A Dosseto, S Turner, J Van-Orman), pp. 125–159. Chichester, UK: Wiley.
167. Costa F, Chakraborty S, Dohmen R. 2003 Diffusion coupling between trace and major elements and a model for calculation of magma residence times using plagioclase. *Geochim. Cosmochim. Acta* **67**, 2189–2200. (doi:10.1016/S0016-7037(02)01345-5)
168. Hartley ME, Morgan DJ, Maclennan J, Edmonds M, Thordarson T. 2016 Tracking timescales of short-term precursors to large basaltic fissure eruptions through Fe–Mg diffusion in olivine. *Earth and Planetary Science Letters* **439**, 58–70. (doi:10.1016/j.epsl.2016.01.018)
169. Cooper KM. 2015 Timescales of crustal magma reservoir processes: insights from U-series crystal ages. *Geol. Soc. Lond. Spec. Publ.* **422**, SP422-7. (doi:10.1144/SP422.7)
170. Cooper KM, Reid MR. 2008 Uranium-series crystal ages. *Rev. Mineral. Geochem.* **69**, 479–544. (doi:10.2138/rmg.2008.69.13)
171. Costa F, Dungan M. 2005 Short time scales of magmatic assimilation from diffusion modeling of multiple elements in olivine. *Geology* **33**, 837–840. (doi:10.1130/G21675.1)
172. Kahl M, Chakraborty S, Costa F, Pompilio M. 2011 Dynamic plumbing system beneath volcanoes revealed by kinetic modeling, and the connection to monitoring data: An example from Mt. Etna. *Earth Planet. Sci. Lett.* **308**, 11–22. (doi:10.1016/j.epsl.2011.05.008)
173. Martin VM, Morgan DJ, Jerram DA, Caddick MJ, Prior DJ, Davidson JP. 2008 Bang! Month-scale eruption triggering at Santorini volcano. *Science* **321**, 1178. (doi:10.1126/science.1159584)
174. Cashman KV. 2004 Volatile controls on magma ascent and eruption. In *The state of the planet: frontiers and challenges in geophysics*, (eds RSJ Sparks, CJ Hawkesworth), pp. 109–124.
175. Edmonds M, Wallace PJ. 2017 Volatiles and exsolved vapor in volcanic systems. *Elements* **13**, 29–34. (doi:10.2113/gselements.13.1.29)
176. Degruyter W, Parmigiani A, Huber C, Bachmann O. 2019 How do volatiles escape their shallow magmatic hearth? *Phil. Trans. R. Soc. A* **377**, 20180017. (doi:10.1098/rsta.2018.0017)
177. Edmonds M, Woods A. 2018 Exsolved volatiles in magma reservoirs. *J. Volcanol. Geotherm. Res.* **368**, 13–30. (doi:10.1016/j.jvolgeores.2018.10.018)
178. Candela PA. 1997 A review of shallow, ore-related granites: textures, volatiles, and ore metals. *J. Petrol.* **38**, 1619–1633. (doi:10.1093/petroj/38.12.1619)
179. Huppert HE, Woods AW. 2002 The role of volatiles in magma chamber dynamics. *Nature* **420**, 493–495. (doi:10.1038/nature01211)
180. Woods AW, Huppert HE. 2003 On magma chamber evolution during slow effusive eruptions. *J. Geophys. Res. Solid Earth* **108**, 2403. (doi:10.1029/2002jb002019)
181. McCormick Kilbride B, Edmonds M, Biggs J. 2016 Observing eruptions of gas-rich compressible magmas from space. *Nat. Commun.* **7**, 13744. (doi:10.1038/ncomms13744)
182. Voight B, Widiwijayanti C, Mattioli G, Elsworth D, Hidayat D, Strutt M. 2010 Magma-sponge hypothesis and stratovolcanoes: case for a compressible reservoir and quasi-steady deep influx at Soufrière Hills Volcano, Montserrat. *Geophys. Res. Lett.* **37**, L00E05. (doi:10.1029/2009gl041732)
183. Husen S, Smith RB, Waite GP. 2004 Evidence for gas and magmatic sources beneath the Yellowstone volcanic field from seismic tomographic imaging. *J. Volcanol. Geotherm. Res.* **131**, 397–410. (doi:10.1016/S0377-0273(03)00416-5)

184. Parmigiani A, Degruyter W, Leclaire S, Huber C, Bachmann O. 2017 The mechanics of shallow magma reservoir outgassing. *Geochem. Geophys. Geosyst.* **18**, 2887–2905. (doi:10.1002/2017GC006912)
185. Parmigiani A, Faroughi S, Huber C, Bachmann O, Su Y. 2016 Bubble accumulation and its role in the evolution of magma reservoirs in the upper crust. *Nature* **532**, 492–495. (doi:10.1038/nature17401)
186. Parmigiani A, Huber C, Bachmann O. 2014 Mush microphysics and the reactivation of crystal-rich magma reservoirs. *J. Geophys. Res. Solid Earth* **119**, 6308–6322. (doi:10.1002/2014JB011124)
187. Oppenheimer J, Rust A, Cashman K, Sandnes B. 2015 Gas migration regimes and outgassing in particle-rich suspensions. *Front. Phys.* **3**, 60. (doi:10.3389/fphy.2015.00060)
188. Cardoso SSS, Woods AW. 1999 On convection in a volatile-saturated magma. *Earth Planet. Sci. Lett.* **168**, 301–310. (doi:10.1016/S0012-821X(99)00057-6)
189. Wallace PJ, Gerlach TM. 1994 Magmatic vapor source for sulfur dioxide released during volcanic eruptions: evidence from Mount Pinatubo. *Science* **265**, 497–499. (doi:10.1126/science.265.5171.497)
190. Wallace PJ, Edmonds M. 2011 The sulfur budget in magmas: evidence from melt inclusions, submarine glasses, and volcanic gas emissions. *Rev. Mineral. Geochem.* **73**, 215–246. (doi:10.2138/rmg.2011.73.8)
191. Wallace PJ. 2005 Volatiles in subduction zone magmas: concentrations and fluxes based on melt inclusion and volcanic gas data. *J. Volcanol. Geotherm. Res.* **140**, 217–240. (doi:10.1016/j.jvolgeores.2004.07.023)
192. Wallace PJ. 2003 From mantle to atmosphere: magma degassing, explosive eruptions, and volcanic volatile budgets. *Dev. Volcanol.* **5**, 105–127. (doi:10.1016/S1871-644X(03)80026-8)
193. Self S. 2006 The effects and consequences of very large explosive volcanic eruptions. *Phil. Trans. R. Soc. A* **364**, 2073–2097. (doi:10.1098/rsta.2006.1814)
194. Christopher T, Edmonds M, Humphreys M, Herd RA. 2010 Volcanic gas emissions from Soufrière Hills Volcano, Montserrat 1995–2009, with implications for mafic magma supply and degassing. *Geophys. Res. Lett.* **37**, L00E04. (doi:10.1029/2009gl041325)
195. Huber C, Bachmann O, Vigneresse JL, Dufek J, Parmigiani A. 2012 A physical model for metal extraction and transport in shallow magmatic systems. *Geochem. Geophys Geosyst.* **13**, Q08003. (doi:10.1029/2012gc004042)
196. Hutchison W *et al.* 2016 Causes of unrest at silicic calderas in the East African Rift: New constraints from InSAR and soil-gas chemistry at Aluto volcano, Ethiopia. *Geochem. Geophys. Geosyst.* **17**, 3008–3030. (doi:10.1002/2016GC006395)
197. Chiodini G, Caliro S, De Martino P, Avino R, Gherardi F. 2012 Early signals of new volcanic unrest at Campi Flegrei caldera? Insights from geochemical data and physical simulations. *Geology* **40**, 943–946. (doi:10.1130/G33251.1)
198. Girona T, Costa F, Newhall C, Taisne B. 2014 On depressurization of volcanic magma reservoirs by passive degassing. *J. Geophys. Res. Solid Earth* **119**, 8667–8687. (doi:10.1002/2014JB011368)
199. Burgisser A, Alletti M, Scaillet B. 2015 Simulating the behavior of volatiles belonging to the C–O–H–S system in silicate melts under magmatic conditions with the software D-Compress. *Comput. Geosci.* **79**, 1–14. (doi:10.1016/j.cageo.2015.03.002)
200. Koleszar AM, Saal AE, Hauri EH, Nagle AN, Liang Y, Kurz MD. 2009 The volatile contents of the Galapagos plume; evidence for H_2O and F open system behavior in melt inclusions. *Earth Planet. Sci. Lett.* **287**, 442–452. (doi:10.1016/j.epsl.2009.08.029)
201. Longpré M-A, Stix J, Klügel A, Shimizu N. 2017 Mantle to surface degassing of carbon-and sulphur-rich alkaline magma at El Hierro, Canary Islands. *Earth Planet. Sci. Lett.* **460**, 268–280. (doi:10.1016/j.epsl.2016.11.043)
202. Métrich N, Bertagnini A, Di Muro A. 2009 Conditions of magma storage, degassing and ascent at Stromboli: new insights into the volcano plumbing system with inferences on the eruptive dynamics. *J. Petrol.* **51**, 603–626. (doi:10.1093/petrology/egp083)
203. Spilliaert N, Allard P, Métrich N, Sobolev A. 2006 Melt inclusion record of the conditions of ascent, degassing, and extrusion of volatile-rich alkali basalt during the powerful 2002 flank eruption of Mount Etna (Italy). *J. Geophys. Res. Solid Earth*, **111**, B04203. (doi:10.1029/2005jb003934)

204. De Maisonneuve CB, Dungan M, Bachmann O, Burgisser A. 2012 Insights into shallow magma storage and crystallization at Volcán Llaima (Andean Southern Volcanic Zone. *Chile). J. Volcanol. Geotherm. Res.* **211**, 76–91. (doi:10.1016/j.jvolgeores.2011.09.010)
205. Ruth DC, Cottrell E, Cortés JA, Kelley KA, Calder ES. 2016 From passive degassing to violent strombolian eruption: the case of the 2008 eruption of Llaima volcano, Chile. *J. Petrol.* **57**, 1833–1864.
206. Sisson T, Layne G. 1993 H_2O in basalt and basaltic andesite glass inclusions from four subduction-related volcanoes. *Earth Planet. Sci. Lett.* **117**, 619–635. (doi:10.1016/0012-821X(93)90107-K)
207. Roggensack K. 2001 Unraveling the 1974 eruption of Fuego volcano (Guatemala) with small crystals and their young melt inclusions. *Geology* **29**, 911–914. (doi:10.1130/0091-7613(2001)029<0911:UTEOFV>2.0.CO;2)
208. Berlo K, Stix J, Roggensack K, Ghaleb B. 2012 A tale of two magmas, Fuego, Guatemala. *Bull. Volcanol.* **74**, 377–390. (doi:10.1007/s00445-011-0530-8)
209. Lloyd AS, Ferriss E, Ruprecht P, Hauri EH, Jicha BR, Plank T. 2016 An assessment of clinopyroxene as a recorder of magmatic water and magma ascent rate. *J. Petrol.* **57**, 1865–1886. (doi:10.1093/petrology/egw058)
210. Annen C, Blundy J, Sparks R. 2006 The genesis of intermediate and silicic magmas in deep crustal hot zones. *J. Petrol.* **47**, 505–539. (doi:10.1093/petrology/egi084)
211. Solano J, Jackson M, Sparks R, Blundy J, Annen C. 2012 Melt segregation in deep crustal hot zones: a mechanism for chemical differentiation, crustal assimilation and the formation of evolved magmas. *J. Petrol.* **53**, 1999–2026. (doi:10.1093/petrology/egs041)
212. Petford N, Gallagher K. 2001 Partial melting of mafic (amphibolitic) lower crust by periodic influx of basaltic magma. *Earth Planet. Sci. Lett.* **193**, 483–499. (doi:10.1016/S0012-821X(01)00481-2)
213. Hildreth W. 1981 Gradients in silicic magma chambers: implications for lithospheric magmatism. *J. Geophys. Res. Solid Earth* **86**, 10 153–10 192. (doi:10.1029/JB086iB11p10153)
214. Ague JJ, Brimhall GH. 1987 Granites of the batholiths of California: products of local assimilation and regional-scale crustal contamination. *Geology* **15**, 63–66. (doi:10.1130/0091-7613(1987)15<63:GOTBOC>2.0.CO;2)
215. Hildreth W, Halliday AN, Christiansen RL. 1991 Isotopic and chemical evidence concerning the genesis and contamination of basaltic and rhyolitic magma beneath the Yellowstone Plateau volcanic field. *J. Petrol.* **32**, 63–138. (doi:10.1093/petrology/32.1.63)
216. Karakas O, Degruyter W, Bachmann O, Dufek J. 2017 Lifetime and size of shallow magma bodies controlled by crustal-scale magmatism. *Nat. Geosci.* **10**, 446. (doi:10.1038/ngeo2959)
217. De Silva S. 2008 Arc magmatism, calderas, and supervolcanoes. *Geology* **36**, 671–672. (doi:10.1130/focus082008.1)
218. Schleicher JM, Bergantz GW, Breidenthal RE, Burgisser A. 2016 Time scales of crystal mixing in magma mushes. *Geophys. Res. Lett.* **43**, 1543–1550. (doi:10.1002/2015GL067372)
219. Woods A, Stock MJ. 2019 Some fluid mechanical constraints on crystallisation and recharge within sills. *Phil. Trans. R. Soc. A* **377**, 20180007. (doi:10.1098/rsta.2018.0007)
220. Pritchard ME, Mather TA, McNutt SR, Delgado FJ, Reath K. 2019 Thoughts on the criteria to determine the origin of volcanic unrest as magmatic or non-magmatic. *Phil. Trans. R. Soc. A* **377**, 20180008. (doi:10.1098/rsta.2018.0008)
221. McNutt SR. 1996 Seismic monitoring and eruption forecasting of volcanoes: a review of the state-of-the-art and case histories. In *Monitoring and mitigation of volcano hazards*, (eds R Scarpa, RI Tilling), pp. 99–146. Berlin, Germany: Springer.
222. Tarasewicz J, White RS, Woods AW, Brandsdóttir B, Gudmundsson MT. 2012 Magma mobilization by downward-propagating decompression of the Eyjafjallajökull volcanic plumbing system. *Geophys. Res. Lett.* **39**. (doi:10.1029/2012gl053518)
223. Scandone R, Cashman KV, Malone SD. 2017 Magma supply, magma ascent and the style of volcanic eruptions. *Earth and Planetary Science Letters* 253, 513–529.
224. Eaton J, Richter D, Krivoy H. 1987 Cycling of magma between the summit reservoir and Kīlauea Iki lava lake during the 1959 eruption of Kīlauea volcano. *U.S. Geol. Surv. Prof. Pap.* **1350**, 1307–1335.
225. Cashman KV, Giordano G. 2014 Calderas and magma reservoirs. *J. Volcanol. Geotherm. Res.* **288**, 28–45.

226. Swallow EJ, Wilson CJ, Myers ML, Wallace PJ, Collins KS, Smith EG. 2018 Evacuation of multiple magma bodies and the onset of caldera collapse in a supereruption, captured in glass and mineral compositions. *Contributions to Mineralogy and Petrology* **173**, 33.
227. Biggs J, Wright T, Lu Z, Parsons B. 2007 Multi-interferogram method for measuring interseismic deformation: Denali Fault, Alaska. *Geophys. J. Int.* **170**, 1165–1179. (doi:10.1111/j.1365-246X.2007.03415.x)
228. Rivalta E, Segall P. 2008 Magma compressibility and the missing source for some dike intrusions. *Geophys. Res. Lett.* **35**, L04306. (doi:10.1029/2007GL032521)
229. Hamlyn J *et al.* 2018 What causes subsidence following the 2011 eruption at Nabro (Eritrea)? *Progress Earth Planet. Sci.* **5**, 31. (doi:10.1186/s40645-018-0186-5)
230. Del Negro C, Currenti G, Scandura D. 2009 Temperature-dependent viscoelastic modeling of ground deformation: application to Etna volcano during the 1993–1997 inflation period. *Phys. Earth Planet. Inter.* **172**, 299–309. (doi:10.1016/j.pepi.2008.10.019)
231. Dragoni M, Magnanensi C. 1989 Displacement and stress produced by a pressurized, spherical magma chamber, surrounded by a viscoelastic shell. *Phys. Earth Planet. Inter.* **56**, 316–328. (doi:10.1016/0031-9201(89)90166-0)
232. Segall P. 2016 Repressurization following eruption from a magma chamber with a viscoelastic aureole. *J. Geophys. Res. Solid Earth* **121**, 8501–8522. (doi:10.1002/2016JB013597)
233. Rae A, Edmonds M, Morgan DJ, Kahl M, Houghton BF, Maclennan J. 2016 Timescales of magma mixing prior to and during the 1959 Kilauea Iki eruption. *Geology* **44**, 463–466. (doi:10.1130/G37800.1)
234. Saunders K, Blundy J, Dohmen R, Cashman K. 2012 Linking petrology and seismology at an active volcano. *Science* **336**, 1023–1027. (doi:10.1126/science.1220066)
235. Sutton AJ, Elias T, Gerlach TM, Stokes JB. 2001 Implications for eruptive processes as indicated by sulfur dioxide emissions from Kı̄lauea Volcano, Hawai'i, 1979–1997. *J. Volcanol. Geotherm. Res.* **108**, 283–302. (doi:10.1016/S0377-0273(00)00291-2)
236. Allard P, Behncke B, D'Amico S, Neri M, Gambino S. 2006 Mount Etna 1993–2005: anatomy of an evolving eruptive cycle. *Earth Sci. Rev.* **78**, 85–114. (doi:10.1016/j.earscirev.2006.04.002)
237. Allard P *et al.* 2016 Prodigious emission rates and magma degassing budget of major, trace and radioactive volatile species from Ambrym basaltic volcano, Vanuatu island Arc. *J. Volcanol. Geotherm. Res.* **322**, 119–143. (doi:10.1016/j.jvolgeores.2015.10.004)
238. Aiuppa A, Federico C, Giudice G, Giuffrida G, Guida R, Gurrieri S, Liuzzo M, Moretti R, Papale P. 2009 The 2007 eruption of Stromboli volcano: insights from real-time measurement of the volcanic gas plume CO_2/SO_2 ratio. *J. Volcanol. Geotherm. Res.* **182**, 221–230. (doi:10.1016/j.jvolgeores.2008.09.013)
239. Burton M, Allard P, Muré F, La Spina A. 2007 Magmatic gas composition reveals the source depth of slug-driven Strombolian explosive activity. *Science* **317**, 227–230. (doi:10.1126/science.1141900)
240. Allard P. 1997 Endogenous magma degassing and storage at Mount Etna. *Geophys. Res. Lett.* **24**, 2219–2222. (doi:10.1029/97GL02101)
241. Menand T, Phillips JC. 2007 Gas segregation in dykes and sills. *J. Volcanol. Geotherm. Res.* **159**, 393–408. (doi:10.1016/j.jvolgeores.2006.08.003)
242. Belien IB, Cashman KV, Rempel AW. 2010 Gas accumulation in particle-rich suspensions and implications for bubble populations in crystal-rich magma. *Earth Planet. Sci. Lett.* **297**, 133–140. (doi:10.1016/j.epsl.2010.06.014)
243. Edmonds M, Oppenheimer C, Pyle D, Herd R, Thompson G. 2003 SO_2 emissions from Soufrière Hills Volcano and their relationship to conduit permeability, hydrothermal interaction and degassing regime. *J. Volcanol. Geotherm. Res.* **124**, 23–43. (doi:10.1016/S0377-0273(03)00041-6)
244. Edmonds M, Pyle D, Oppenheimer C. 2001 A model for degassing at the Soufrière Hills Volcano, Montserrat, West Indies, based on geochemical data. *Earth Planet. Sci. Lett.* **186**, 159–173. (doi:10.1016/S0012-821X(01)00242-4)
245. Anderson KR, Poland MP. 2016 Bayesian estimation of magma supply, storage, and eruption rates using a multiphysical volcano model: Kīlauea Volcano, 2000–2012. *Earth Planet. Sci. Lett.* **447**, 161–171. (doi:10.1016/j.epsl.2016.04.029)